SKI Report 01:11

Research

Chemical Buffering in Natural and Engineered Barrier Systems: Thermodynamic Constraints and Performance Assessment Consequences

Randolph C. Arthur
Wei Zhou

December 2000

ISSN 1104-1374
ISRN SKI-R-01/11-SE

SKI Report 01:11

Research

Chemical Buffering in Natural and Engineered Barrier Systems: Thermodynamic Constraints and Performance Assessment Consequences

Randolph C. Arthur
Wei Zhou

Monitor Scientific, LLC
3900 S. Wadsworth Blvd., Suite 555
Denver, Colorado 80235
USA

December 2000

SKI Project Number 98240

SKI perspective

The KBS-3 concept for final disposal of spent nuclear fuel is based on isolation of the fuel within copper-canisters, surrounded by a layer of bentonite clay (the engineered barrier system). The evolution of the chemical environment in the vicinity of the copper-canisters must the addressed in the evaluation of the long-term safety. This is because solubility and sorption behavior of many radionuclides as well as engineered barrier stability may be sensitive to the chemical environment.

Bentonite clay does not exist naturally in the geochemical environment of the Swedish bedrock. The pore-water composition within bentonite can therefore not be expected to be identical to the groundwater composition in the bedrock. This difference may persist for long time periods, due to a very slow mass transfer and depend on the chemical buffering capacity of bentonite. The goal with the present study is to develop an approach to account for this buffering capacity. The quantification of this capacity in a system with several heterogeneous reactions with different kinetics is not a trivial task.

The pore-water pH may be slightly higher within the buffer as compared to the groundwater depending on site specific circumstances. This study shows that the difference will persist for at least several thousand years. A pH front is expected to develop within the buffer, which is moving at a rate inversely proportional to the buffering capacity. A conclusive prediction of the pH front movement can not be made at present, however, due to uncertainties in the kinetics of reactions involving aluminosilicate phases.

It needs to be emphasized that all phenomena of importance for the evolution of the pore-water chemistry can not be included in a single modeling approach. SKI therefore suggests that it might be possible to develop alternative modeling approaches that could complement the present study. Other aspects of chemical buffering in addition to pH effects needs to be considered (ionic strength effects, influence of conservative solutes etc.). Furthermore, it is obvious that the assumptions concerning aluminosilicate reaction kinetics needs to be scrutinized, due to its potentially large capacity for chemical buffering.

Stockholm, March 21, 2001

Bo Strömberg

Summary

Thermodynamic and kinetic constraints on the chemical buffering properties of natural and engineered-barrier systems are derived in this study from theoretical descriptions, incorporated in the reaction-path model, of reversible and irreversible mass transfer in multicomponent, multiphase systems. The buffering properties of such systems are conditional properties because they refer to a specific aqueous species in a system that is open with respect to a specific reactant. The solution to a mathematical statement of this concept requires evaluation of the dependence of the activity of the buffered species on incremental changes in the overall reaction-progress variable. This dependence can be represented by a truncated Taylor's series expansion, where the values of associated derivatives are calculated using finite-difference techniques and mass-balance, charge-balance and mass-action constraints. Kinetic constraints on buffering behavior can also be described if the relation between reactant flux and reaction rate is well defined. This relation is explicit for the important case of advective groundwater flow and water-rock interaction.

We apply the theoretical basis of the chemical buffering concept to processes that could affect the performance of a deep geologic repository for nuclear waste. Specifically, we focus on the likelihood that an inverse relation must exist between the buffer intensity and the migration velocity of reaction fronts in systems involving advective or diffusive mass transport. A quantitative understanding of this relation would provide the basis for evaluating the potential role of chemical buffering in achieving the isolation and retardation functions of the EBS and geosphere in a KBS-3 repository.

Our preliminary evaluation of this role considers the effects of chemical buffering on the propagation velocity of a pH front in both the near- and far field. We use a geochemical modeling technique compatible with the reaction-path model to simulate the acidimetric/ alkalimetric titration of pore solutions equilibrated with water-saturated, compacted MX-80 bentonite. Calculation of the inverse of derivatives of the simulated titration curve provides estimates of the pH buffer intensity. Analytical and adaptive-grid numerical models are then used to simulate the propagation velocity of the pH front through the buffer. Two assumptions that are adopted in these models may be questionable, however: 1) that the region near the pH front is a closed chemical system, and 2) that local and partial equilibrium is sustained as H^+ diffuses into this region. A rigorous reactive-transport modeling approach may be needed to assess the validity of these assumptions.

A reaction-path model appropriate for advection-dominated groundwater flow in one spatial dimension is also used in this study to evaluate the relation between chemical buffering due to water-rock interaction and the migration velocity of a pH front in a granitic host rock. The modeling approach is based on the stationary state approximation to the governing mass-transport equations controlling coupled fluid flow and water-rock interaction. A consequence of stationary-state behavior is that the migration velocity of a reaction front is fixed relative to the Darcy flow velocity. An analytical expression consistent with this behavior predicts that front velocities are attenuated relative to the flow velocity by a retardation factor, which is similar, and in some cases identical, to the buffer intensity of reactions that control the front. A key assumption in this model is that the groundwater system involves purely advective

transport in a homogeneous porous medium. This may be unrealistic in real groundwater systems, except over extremely limited scales of space and time.

Results of both the near-field and far-field models indicate that buffering may strongly attenuate the migration velocities of reaction fronts, and that front velocities are inversely proportional to the buffer intensity. For conditions considered in the bentonite model, calculated front velocities vary from 6.6 x 10^{-2} to 6.6 x 10^{-5} mm yr^{-1}, corresponding to values of the buffer intensity between 1 and 1000 meq l^{-1}, respectively. Corresponding travel times for the front to migrate from the buffer-host rock interface to the buffer-canister boundary range from about 5 x 10^{3} to 5 x 10^{6} years. For conditions considered in the far-field model, the estimated pH-front velocity is about 5.7 x 10^{-1} mm yr^{-1}, or a factor 5.7 x 10^{-5} slower than the assumed Darcy flow velocity of 10 m yr^{-1}. The corresponding time for the front to migrate 500 m (*e.g.*, from the ground surface to the depth of a KBS-3 repository) is about 9 x 10^{5} years.

With the preliminary nature of these results in mind, we conclude that chemical buffering may play an important role in determining the performance of a KBS-3 repository. For example, periods of time that are significant in relation to performance-assessment time scales may be required for a pH front, and perhaps other types of fronts, to migrate from the buffer-host rock boundary to the buffer-canister boundary (just 35 cm in width). This implies that the KBS-3 near field could in effect be decoupled from the far field, thus minimizing effects on repository performance of time-dependent variations in the geosphere. Similarly, buffering may strongly resist changes in the chemistry of the geosphere, which could be caused, for example, by future variations in climate or other natural or man-induced processes.

Sammanfattning

I denna studie härleds termodynamiska och kinetiska begränsningar för kemisk buffring i naturliga och tekniska barriärer, från teoretiska beskrivningar av en reaktionsvägsmodell som beskriver reversibel respektive irreversibel materieöverföring i ett system med flera komponenter och faser. Buffringsegenskaperna i ett sådant system är villkorsberoende eftersom de utgår från en specifik komponent i vattenfasen i ett system som är öppet relativt en specifik reaktant. Den matematiska lösningen av detta koncept kräver en utvärdering av beroendet av aktiviteten hos de buffrande komponenter vid stegvisa ändringar hos den övergripande reaktionsvägsvariabeln. Detta beroende kan representeras av ett stympat utryck av en Taylor-utveckling, i vilket värdena av associerade derivator beräknas med finita differensmetoden, massbalanser, laddningsbalanser och massverkansutryck. Kinetiska begränsningar för kemisk buffring kan också beskrivas om relationen mellan reaktantflux och reaktionshastighet är väldefinierad. Denna relation är explicit för det viktiga fallet med advektivt grundvattenflöde och växelverkan mellan grundvatten och bergets mineral.

Vi tillämpar här den teoretiska grunden för kemisk buffring på processer som kan påverka funktionen av ett geologiskt slutförvar för kärnavfall. Mer specifikt fokuserar vi oss på sannolikheten för att ett omvänt förhållande råder mellan intensiteten av kemisk buffring och transporthastigheten av en reaktionsfront i ett system som inbegriper advektiv och diffusiv materietransport. En kvantitativ förståelse för denna relation skulle ge en bas för att utvärdera den potentiella rollen av kemisk buffring för att uppnå isolerande och retarderande funktioner hos de tekniska barriärerna och geosfären i ett slutförvar av KBS-3 typ.

Vår preliminära utvärdering av denna roll tar hänsyn till effekterna av kemisk buffring med avseende på den hastighet med vilken en pH-front förflyttar sig både i när- och fjärrområdet kring ett slutförvar. Vi använder oss av en geokemisk modelleringsmetod som är kompatibel med reaktionsvägsmodellen för att simulera den acidimetriska resp. alkalimetriska titreringen av porvattenlösningar jämviktade med en vattenmättad och kompakterad MX-80 bentonit. Beräkningar av inversen för derivatan av den simulerade titreringskurvan ger en uppskattning av pH-buffringsintensiteten. Analytiska modeller och numeriska modeller med anpassningsbar grid används för att simulera hasigheten med vilken en pH front förflyttar sig genom bufferten. Två antaganden som används i dessa modeller är dock diskutabla: 1) regionen alldeles i närheten av pH-fronten betraktas som ett slutet system, och 2) lokal och partiell jämvikt upprätthålls när H^+-joner diffunderar in i denna region. En rigorös metod baserad på modellering av reaktiv transport skulle erfordras för att utvärdera giltigheten av de två ovanstående antagandena.

En reaktionsvägsmodell användbar för grundvattenflöde dominerat av advektion i en rumslig dimension används också i denna studie för att utvärdera relationen mellan kemisk buffring orsakad av reaktioner mellan grundvatten och bergets mineral och migrationshastigheten av en pH-front i granitiskt berg. Den utnyttjade metoden baseras på en approximation utgående från stationära tillstånd, som tillämpas på masstransport ekvationer som kontrollerar kopplat flöde och reaktioner mellan grundvatten och berg. En konsekvens av användandet av stationära tillstånd är att migrationshastigheten av en reaktionsfront är fixerad relativt Darcy flödeshastigheten. Ett analytiskt uttryck,

formulerat för att vara konsistent med ett sådant beteende, förutsäger att fronthastigheten bromsas relativt flödeshastigheten med en retardationsfaktor, som liknar och i vissa fall är identisk med buffringsintensiteten för de kemiska reaktionerna som kontrollerar fronten. Ett nyckelantagande i denna modell är att transport i grundvattensystemet endast inkluderar advektion i ett homogent poröst medium. Detta är orealistiskt för ett verkligt grundvattensystem, utom för mycket begränsade tids- och längdskalor.

Resultat från de båda modeller som beskriver både när- och fjärrområdet, tyder på att materialens buffringsegenskaper starkt begränsar rörelsen av reaktionsfronter och att fronthastigheterna är omvänt proportionella mot buffringsintensiteten. För de förutsättningar som beaktats vid formulering av bentonitmodellen, beräknas fronthastigheten variera mellan $6.6x10^{-2}$ till $6.6x10^{-5}$ mm per år, vilket motsvarar värden av buffringsintensiteten mellan 1 respektive 1000 meq per liter. Motsvarande transporttider för fronten att migrera från gränsskiktet mellan buffert och berg till gränsskiktet mellan buffert och kapsel är $5x10^{3}$ till $5x10^{6}$ år. För de förutsättningar som beaktats vid formulering av modellen för fjärrområdet, är den beräknade hastigheten för pH-fronten ungefär $5.7x10^{-1}$ mm per år, eller en faktor $5.7x10^{-5}$ långsammare än den antagna Darcy flödeshastigheten av 10 m per år. Tiden för fronten att röra sig 500 m (t.ex. från markytan till ett KBS-3 förvar) är ungefär $9x10^{5}$ år.

Med dessa preliminära resultat i åtanke drar vi slutsatsen att kemisk buffring är av stor betydelse för att bestämma ett KBS-3 förvars egenskaper. Till exempel, tidsperioder som är av betydelse i relation till tidsskalor i säkerhetsanalyser kan erfordras för att pH fronten skall röra sig från gränsskiktet mellan buffert och berg till gränsskiktet mellan buffert och kapsel (som bara är 35 cm bred). Detta indikerar att närområdet kring ett KBS-3 förvar kan i själva verket kopplas isär från fjärrområdet, vilket minimerar inverkan av tidberoende variationer i geosfären. På samma sätt kan buffring motverka förändringar av de kemiska betingelserna i geosfären, vilka till exempel skulle kunna orsakas av framtida variationer i klimat eller andra av människan påverkade processer.

Table of Contents

1 Introduction

Chemical buffering is an implicit concept in safety assessments of the KBS-3 repository for spent nuclear fuel. In the most general terms, chemical buffering refers to the ability of a chemical system to resist change in one or more intensive properties resulting from a change in corresponding extensive properties as energy and/or mass is transferred across the system's boundaries (Anderson and Crerar, 1993). The notion of a certain resistance to change is included in the KBS-3 performance function of the host rock to provide a stable geochemical environment over long periods of time, such that the long-term performance of the engineered barrier system (EBS) is not jeopardized (SKB, 1992). Chemical buffering is similarly implied by the isolation function of EBS components to "resist chemical transformation", their retardation function to "resist chemical alteration", and their favorable properties to "stabilize the chemical environment" (SKB, 1995).

The effects on repository performance of time-dependent variations in geosphere properties, which are evaluated in the SITE-94 (SKI, 1996) and SR 97 (SKB, 1999) performance assessments, may also be considered in terms of the chemical buffering properties of geologic and engineered barrier systems. For example, if the host rocks in a KBS-3 repository are able to resist changes in groundwater chemistry that could be induced by future variations in climate, then such variations may not significantly impact repository performance[1]. Chemical buffering in this sense is addressed indirectly in a number of modeling studies, which indicate, for example, that granitic rocks similar to those comprising much of the crystalline basement of Sweden would strongly attenuate the migration of redox fronts that could be generated by the downward flow of oxygenated glacial meltwaters (Neretnieks, 1985; Arthur, 1996; Glynn and Voss, 1999; Guimerà *et al.*, 1999). Bruno *et al.* (1999) describe similar investigations that invoke the chemical buffering properties of "impurity" minerals in bentonite.

Despite the implied importance of chemical buffering as evidenced by the statements and studies noted above, there has been little effort to incorporate this concept quantitatively into performance assessments. We believe the underlying reason for this lack of progress stems from the fact that existing models of buffering behavior are incompatible with the multicomponent, multiphase nature of geologic and engineered-barrier systems. For example, the classic chemical model (Sørensen, 1909; Jørgensen, 1955) deals only with homogeneous reactions in an aqueous phase, and is therefore insufficiently general to account for other, heterogeneous reactions that are certain to occur in geologic and engineered-barrier systems (Rosing, 1993). The chemical model has been modified and used in geological studies to help define the fugacities of gases equilibrated with various mineral assemblages in closed systems (Eugster, 1957; Greenwood, 1975). The geological models ignore mass-balance constraints on the buffer capacity, however. Stumm and Morgan (1996) derive analytical expressions that approximate the pH-buffering properties of individual heterogeneous reactions involving carbonate and silicate minerals, but in reality the pH-buffering behavior of geologic systems is controlled by all heterogeneous and homogeneous reactions that include H^+ as a reactant or product. Hutcheon *et al.* (1993) evaluate mass-action

[1] It should be emphasized, however, that the concept of chemical buffering does not apply to inert groundwater constituents (*e.g.*, Cl^-), which may also affect the performance of a repository.

constraints on the pH buffer intensity of individual reactions among stable and metastable silicate phases in sedimentary oil/gas reservoirs, but do not consider associated mass-balance and kinetic constraints. Roaldset *et al.* (1996) and Savage *et al.* (1999) extend this approach to evaluate the pH-buffering properties of bentonite buffers[2] in the KBS-3 EBS. Their approach differs from that of Hutcheon *et al.* (*op. cit.*) because it does not require specification *a priori* of reactions that are pH controlling, and because it accounts for mass-balance constraints on the buffer capacity. Kinetic constraints are dealt with only qualitatively in these latter studies, however.

The present study attempts to establish a scientific basis for incorporation of the chemical buffering concept into performance assessments. As noted above, we believe it is important to first specify how thermodynamic constraints control the chemical buffering properties of natural and engineered-barrier systems. These constraints are therefore derived in Section 2 from existing theoretical descriptions of reversible and irreversible mass transfer in multicomponent, multiphase systems. This theoretical framework is incorporated in several geochemical software packages, which can be used to evaluate buffering behavior. This is demonstrated in Section 3, where the pH buffering properties of bentonite buffer materials are estimated, and where associated attenuation factors limiting the migration velocities of reaction fronts in the buffer and a granitic host rock are calculated.

[2] The term "buffer" as used here does not refer the *chemical* buffering properties of bentonite, although as noted above such properties are implied in the KBS-3 isolation and retardation functions of this material.

2 Theoretical background

The buffering behavior of a system at constant temperature and pressure is defined with respect to a given aqueous species by the change in its activity between an initial and subsequent state of the system characterized by additions to (or losses from) the system of a certain amount of a reactant that affects the concentration of the buffered species. This behavior is characterized by a single parameter, the *buffer sensitivity* (α), defined by equations of the general form (Rosing, 1993):

$$\alpha \equiv \frac{da_k}{dn_f} = \frac{d(\gamma_k m_k)}{dn_f}, \tag{1}$$

where a_k refers to the activity of the *k-th* aqueous species, γ_k and m_k stand for its activity coefficient and molality, respectively, and n_f represents the number of moles of a "fugitive" reactant added to, or abstracted from, the system. The buffer sensitivity is a conditional property of the system because it refers to a specific aqueous species in a system that is open to a specific reactant. The only restriction on the reactant is that its concentration within the system must be independently variable. Reactants thus include thermodynamic components, ionic solutes in an electrolyte solution, minerals, gases, and non-mineral crystalline solids. The inverse of the buffer sensitivity, denoted by the symbol β, is referred to as the *buffer intensity* (Van Slyke, 1922) or *buffer capacity* (Jørgensen, 1955; Rosing, 1993). We adopt the former terminology in the following discussion and reserve the latter for an extensive property of the system (Section 2.2).

Adopting the buffer-sensitivity concept as a starting point, the objective is then to derive a statement of Eqn. (1) that is appropriate for multicomponent, multiphase systems. A suitable theoretical framework for this purpose is described by Helgeson (1968) and others (*e.g.*, Helgeson, 1970, 1972, 1979; Helgeson *et al.*, 1969, 1970; Fritz and Tardy, 1967a,b; Wolery, 1978; Wolery 1992; Bethke, 1996). It is incorporated in the so-called reaction-path model, which takes advantage of thermodynamic constraints imposed by partial and local equilibrium to calculate the extent to which components are redistributed among minerals and an aqueous solution as the solution reacts irreversibly with its mineralogic environment. Partial equilibrium occurs when the system is in equilibrium with at least one chemical process, which can be described by a reversible chemical reaction, but out of equilibrium with respect to others. Local equilibrium occurs in a system when phases that are in contact with one another react reversibly in response to changes in chemical potential. The concept of chemical buffering is compatible with these conditions and constraints because the redistribution of an added reactant's mass among a system's mineral and aqueous phases must result from one or more reactions, which may involve a buffered species as reactant or product.

The approach taken here is to derive a statement of Eqn. (1) that is consistent with the reaction-path model. The equation is described below, followed by an assessment of associated thermodynamic constraints on buffering behavior. Because the main focus of the discussion is on the concept of chemical buffering, relevant aspects of the reaction-path model are introduced with little explanation. The model is described in more detail, however, in the references noted above.

2.1 Calculation of the buffer sensitivity

Reaction-path models describe variations in the activity of an aqueous species relative to changes in a reaction-progress variable, ξ, which in general represents the extent, or degree of advancement, of an overall irreversible process involving one or more reversible and irreversible reactions (DeDonder, 1920; Prigogine, 1955; Helgeson, 1968). Each irreversible reaction in an overall irreversible process has its own associated progress variable, ξ_r. If the rates of these reactions are described in terms of actual rate laws, then the overall reaction-progress variable is itself a function of time. Otherwise it is simply treated as an integration variable.

A statement of Eqn. (1) that is compatible with the reaction-path model is given by:

$$\alpha = \frac{da_k}{d\xi} \Big/ \frac{dn_f}{d\xi}, \tag{2}$$

where both derivatives refer to the same increment of reaction progress, $d\xi$. The denominator in this equation specifies the flux of the reactant into or out of the system, and is therefore largely constrained by the nature of the problem at hand. For example, in a titration process involving addition of a reactant to a system in which the rates of all reactions are sufficiently fast to sustain equilibrium, it is convenient to assume that the flux is given by (Wolery, 1992):

$$\frac{dn_f}{d\xi} = 1, \tag{3}$$

in which case the number of moles of reactant added to the system is numerically equal to the progress variable. An equation analogous to Eqn. (3) for the important case of advective groundwater flow and kinetically controlled water-rock interaction is described in a later section. In any case, once an appropriate correlation between dn_f and $d\xi$ is defined, calculation of the buffer sensitivity then requires calculation of the quantity $da_k/d\xi$.

The functional dependence of a_k on ξ is approximated in the reaction-path model in the form of a truncated Taylor's series expansion (*e.g.*, Wolery, 1992):

$$a_k(\xi) = a_k(\xi_0) + \gamma_k \sum_{x=1}^{y} \frac{1}{x!} \left(\frac{d^x m_k}{d\xi^x} \right)_0 (\Delta\xi)^x, \tag{4}$$

where here it is assumed that γ_k does not vary significantly over the increment of reaction progress. The symbol y in this equation denotes the order of the series, ξ refers to a point of reaction progress, ξ_0 represents the most recent point at which the calculation has been completed, and $\Delta\xi$ (= $\xi - \xi_0$) stands for the current step size in the reaction path.

Differentiation of Eqn. (4) with respect to ξ leads to:

$$\frac{da_k(\xi)}{d\xi} = \gamma_k \sum_{x=1}^{y} \frac{1}{(x-1)!} \left(\frac{d^x m_k}{d\xi^x} \right)_0 (\Delta\xi)^{(x-1)}, \tag{5}$$

which corresponds to a Taylor's expansion of one less order. A solution of this equation determines the value of the numerator in Eqn. (2), from which the buffer sensitivity can be calculated by dividing this value by the denominator evaluated over the same increment of reaction progress. Numerical methods are required to solve Eqn. (5), however, because the derivatives on the right-hand side of this equation include parameters whose numerical values depend on the initial concentrations at ξ_0 of aqueous species and minerals in the system. These are path-dependent variables that cannot be described by exact differentials, but which are closely approximated using finite-difference techniques (Wolery, 1992).

The values of the derivatives in Eqn. (5) are subject to thermodynamic constraints, which thus control the chemical buffering properties of the system. To illustrate how these constraints control buffering behavior, expressions for the first derivative on the right-hand side of Eqn. (5) are derived below from equations describing mass-balance, charge-balance, mass-action and kinetic constraints on mass transfer in multicomponent, multiphase systems. For the sake of clarity, we consider only the first derivative in detail. Derivation of similar expressions for the higher order derivatives is straightforward (Helgeson, 1968).

2.2 Conservation of mass

The extent to which an element is redistributed among the phases of a system open with respect to a single fugitive reactant that contains the element of interest is partially constrained by (Helgeson, 1979; Wolery, 1992):

$$\sum_{\theta} \eta_{\varepsilon,\theta} \frac{dm_\theta}{d\xi} + \sum_{i} \eta_{\varepsilon,i} \frac{dm_i}{d\xi} + \sum_{\pi} \sum_{\upsilon} \eta_{\varepsilon,\upsilon\pi} \frac{dm_{\upsilon\pi}}{d\xi} + \eta_{e,f} \frac{dm_f}{d\xi} = 0, \tag{6}$$

where factors $\eta_{\varepsilon,\theta}$, $\eta_{\varepsilon,i}$, $\eta_{\varepsilon,\upsilon\pi}$ and $\eta_{\varepsilon,f}$ refer to the number of moles of the ε-*th* element in 1 mole of the θ-th stoichiometric mineral, the i-th aqueous species, the υ-th component of the π-th solid solution and the f-th fugitive reactant, respectively. The molality, m, denotes the number of moles of the subscripted mineral, aqueous species, solid solution or reactant in 1 kg H_2O, *i.e.*,:

$$\frac{dm}{d\xi} = \frac{1}{W_{H_2O}} \frac{dn}{d\xi}, \tag{7}$$

where W_{H2O} represents the number of kilograms of H_2O in the system[3].

[3] Conservation of mass in a system undergoing significant evaporation or dilution requires modification of Eqn. (7) to account for variations in the mass of the solvent and associated effects on molality. The reaction-path model uses a Taylor's expansion analogous to Eqn. (4) to calculate variations in the number of moles of H_2O in the system (Helgeson *et al.*, 1970). Molalities are then adjusted accordingly after each increment of reaction progress.

It follows from Eqn. (6) that the first derivative in Eqn. (5) evaluated at ξ_0 for the i-th buffered species distinguished by $i = k$ is given by:

$$\frac{dm_k}{d\xi} = -\frac{1}{\eta_{\varepsilon,k}}\left(\sum_{\theta}\eta_{\varepsilon,\theta}\frac{dm_\theta}{d\xi} + \sum_{i\neq k}\eta_{\varepsilon,i}\frac{dm_i}{d\xi} + \sum_{\pi}\sum_{\upsilon}\eta_{\varepsilon,\upsilon\pi}\frac{dm_{\upsilon\pi}}{d\xi} + \eta_{\varepsilon,f}\frac{dm_f}{d\xi}\right), \tag{8}$$

which thus implies that the buffering properties of complex systems are controlled by mass-balance constraints. This can be seen more clearly by considering a limiting condition in which the mass of the ε-th element of the f-th reactant is not redistributed among any of the minerals and aqueous species in the system other than the k-th buffered species. In this case all but the last derivative terms on the right-hand side of Eqn. (8) are equal to zero, and:

$$\frac{dm^\circ_k}{d\xi} = -\frac{\eta_{\varepsilon,f}}{\eta_{\varepsilon,k}}\frac{dm_f}{d\xi}, \tag{9}$$

where dm°_k refers to the change in molality of the buffered species under these conditions. This change in molality represents the maximum possible change for a given amount of the reactant added to the system. The effects of mass-transfer among other aqueous species and minerals can then be evaluated by dividing Eqn. (8) by Eqn. (9), which results in the following expression:

$$\frac{dm_k}{dm^\circ_k} = \frac{1}{\eta_{\varepsilon,f}}\left(\sum_{\theta}\eta_{\varepsilon,\theta}\frac{dm_\theta}{dm_f} + \sum_{i\neq k}\eta_{\varepsilon,i}\frac{dm_i}{dm_f} + \sum_{\pi}\sum_{\upsilon}\eta_{\varepsilon,\upsilon\pi}\frac{dm_{\upsilon\pi}}{dm_f} + \eta_{\varepsilon,f}\right) \tag{10}$$

Thus, because $dm_k/dm^\circ_k \leq 1$, the cumulative effect of redistribution of the reactant's mass among other aqueous species and minerals in the system, given by the terms within the parentheses on the right-hand side of this equation, is to minimize, or to "dampen", changes in the molality of the buffered species (Rosing, 1993).

The derivatives appearing in Eqn. (8) for stoichiometric minerals and solid solutions may be discontinuous because these solids may dissolve completely, or new solids may precipitate, over an interval of reaction progress. The mass-balance constraint imposed by this equation is thus an extensive property of the system because the quantity $dm_k/d\xi$ depends in part on the number of moles of stoichiometric phases and solid solutions present in the system at ξ_0. Should any of these minerals dissolve completely over the subsequent increment of reaction progress, or should any new phases precipitate, then a discontinuity may result between values of $dm_k/d\xi$ evaluated at ξ_0 and ξ. As will be seen, similar discontinuities may also occur among associated parameters such as the buffer sensitivity and buffer intensity. To account for this aspect of buffering behavior, we use the term *buffer capacity* to refer to the number of moles per kilogram H_2O of a given mineral that is subject to dissolution or precipitation reactions induced by addition of a reactant to the system. Thus the buffer capacity of a system responding to changes in pH by dissolution of calcite, for example, is defined by the molal concentration of calcite at ξ_0. If the changes in pH are caused by addition of a strong acid to the system in a titration process, then the total buffer capacity of the system with respect to calcite is determined by the initial molality of this mineral prior to titration.

2.3 Conservation of charge

The buffering properties of a system are also controlled by charge-balance constraints, represented by (Helgeson, 1968):

$$\sum_i Z_i \frac{dm_i}{d\xi} = 0, \tag{11}$$

where Z_i refers to the charge on the i-th aqueous species. The first derivative in Eqn. (5), again evaluated at ξ_0 for the i-th aqueous species distinguished by $i = k$, is therefore also constrained by:

$$\frac{dm_k}{d\xi} = -\sum_{i \neq k} \frac{Z_i}{Z_k} \frac{dm_i}{d\xi}. \tag{12}$$

Conservation of charge thus constrains the buffering properties of a system because it requires that any change in concentration of an ionic buffered species must be compensated by changes in the concentrations of other ions of the same or opposite charge.

2.4 Law of mass action

Reversible mass transfer between stoichiometric minerals and/or aqueous species restricts relative changes in the activities of the species to those compatible with:

$$\sum_i \nu_{i,r} \ln a_i = \sum_i \nu_{i,r} \ln m_i + \sum_i \nu_{i,r} \ln \gamma_i = \ln K_r, \tag{13}$$

where $\nu_{i,r}$ denotes the stoichiometric reaction coefficient for the i-th aqueous species in the r-th reaction (positive for products and negative for reactants) and K_r stands for the corresponding equilibrium constant. Similar constraints for reactions involving a solid solution are described by Helgeson *et al.* (1970). In either case, the change in activity of a reactant or product species during an irreversible process causing the system to change from an initial to a subsequent state of partial and local equilibrium can be described by differentiating Eqn. (13), or analogous equations for reactions involving solid solutions, with respect to the reaction-progress variable at constant temperature and pressure [see Helgeson (1979) for the general case of variable temperature and/or pressure]:

$$\sum_i \nu_{i,r} \frac{d \ln a_i}{d\xi} = \sum_i \left(\nu_{i,r} \frac{d \ln m_i}{d\xi} + \nu_{i,r} \frac{d \ln \gamma_i}{d\xi} \right) = \frac{d \ln K_r}{d\xi} = 0. \tag{14}$$

If, as assumed earlier, changes in the activity coefficients are negligible over the increment of reaction progress, Eqn. (14) simplifies to:

$$\sum_i \nu_{i,r} \frac{d \ln m_i}{d\xi} = 0. \tag{15}$$

Mass-action constraints on variations in the molality of a given aqueous species, distinguished by $i = k$, imposed by reversible equilibrium is then given by:

$$\frac{d\ln m_k}{d\xi} = -\sum_{i \neq k} \frac{\nu_{i,r}}{\nu_{k,r}} \frac{d\ln m_i}{d\xi}, \text{ or} \tag{16}$$

$$\frac{dm_k}{d\xi} = -m_k \sum_{i \neq k} \frac{\nu_{i,r}}{\nu_{k,r}} \frac{d\ln m_i}{d\xi}, \tag{17}$$

where the parameter m_k on the right-hand side of the latter equation refers to the molality of the k-th species in the initial state of the system at ξ_0.

Reversible mass transfer between stoichiometric minerals, solid solutions and/or aqueous species governs the buffering properties of a system independently of mass-balance and charge-balance constraints. The buffering constraint represented by Eqn. (17) differs from that imposed by Eqn. (8), for example, because aqueous species in the former equation are not limited to those containing a given element. In other words, the buffering properties of multicomponent, multiphase systems are controlled not only by the redistribution of a reactant's mass among various phases, but also by mass transfer involving other components in the system (Rosing, 1993).

2.5 Kinetic constraints

Mass-action constraints imposed by reversible equilibrium require that the flux of a fugitive reactant through the system's boundaries is slow enough to allow equilibrium to be maintained. If the flux is too fast, then buffering is controlled both by the flux and kinetic constraints on the rates of one or more reactions. The relation between flux and reaction rate then in effect constitutes an additional degree of freedom on the buffering behavior of the system.

Kinetic constraints on the buffering properties of a system cannot be determined if the relation between flux and reaction rate is ill defined. Wieland *et al.* (1994), for example, use a potentiometric titration technique to measure the change in pH of a suspension of Na-montmorillonite following incremental additions to the suspension of a strong acid (HNO_3) or strong base (NaOH). Although the primary objective of these experiments was to measure the adsorption of H^+ by montmorillonite, the experimental data could also be used to construct a titration curve showing the change in pH versus the change in number of mol l^{-1} of strong acid or base added to the system. For the acid-titration data, the negative slope of the titration curve would then define the pH buffer sensitivity, and the negative inverse of this slope would define the buffer intensity (*e.g.*, Stumm and Morgan, 1996). Wieland *et al.* (*op. cit.*) arbitrarily assume that ten minutes is sufficient time between each incremental addition of the acid solution for hydrogen ions to sorb onto the surface of montmorillonite. Unfortunately, this assumption is incompatible with limited experimental data (Heydemann, 1966; May *et al.*, 1986; Furrer *et al.*, 1993; Cama *et al.*, 1994; Cama *et al.*, 2000) suggesting that time intervals

as long as about four years may be required for montmorillonite to equilibrate with an aqueous solution (Nagy, 1994). The experimental results reported by Wieland *et al.* (*op. cit*) therefore apparently refer to an unknown stage of reaction progress corresponding to partial irreversible dissolution of montmorillonite in response to periodic changes in the concentration of H^+. The understanding that can be gleaned from these data of the pH buffering properties of Na-montmorillonite is thus qualitative at best.

In contrast, the relation between flux and reaction rate is explicit for the case of advective groundwater flow and water-rock interaction. Adopting the generally realistic assumption that homogeneous reactions between aqueous species are sufficiently fast to sustain local equilibrium within the fluid phase, the chemical evolution of the groundwater is then controlled by the fluid-flow rate and the rates of heterogeneous mineral-fluid reactions. A "packet" of fluid representing a given volume of groundwater is thus open with respect to the minerals it encounters along the flow path. From the point of view of an observer at rest with the fluid packet, dissolution of a mineral causes the mineral's components to continuously enter the packet at a rate determined by the kinetics of the reaction and the period of time the packet is in contact with the mineral. Conversely, precipitation over the same time interval may cause another mineral's components to continuously exit the fluid packet at a rate determined by the rate of the precipitation reaction. Associated variations in the activity of an aqueous species within the packet resulting from the net change in the number of moles of a given reactant added to, or lost from, the fluid by mineral dissolution and/or precipitation then determines the buffer sensitivity of that species with respect to the groundwater flow velocity and mineral-fluid reaction rates. The net flux of a reactant under these conditions is thus itself determined by reaction kinetics and the fluid-flow velocity.

Because coupled processes involving groundwater flow and water-rock interaction are expected to partially control the chemical evolution of groundwaters circulating through host rocks in a KBS-3 repository, it is important to evaluate associated kinetic constraints on the buffering behavior of such systems. Our evaluation is based on the so-called stationary-state approximation to coupled fluid flow and water-rock interaction, which requires a few introductory remarks describing key aspects of this model. Practical limitations in applying this model to natural systems are discussed by Arthur *et al.* (2000).

2.5.1 Stationary-state approximation

The stationary state approximation (Lichtner 1985; 1988) represents the evolution of chemical conditions in open multicomponent, multiphase systems in terms of a sequence of relatively long-lived stationary states of the system, which are linked in time by short-lived transients. Each stationary state is represented by spatially fixed reaction boundaries, and nearly constant mineral abundances, porosity, permeability, and reactive surface areas. A stationary state is an open-system analogue of an equilibrium state in closed systems insofar as both are independent of time. A stationary state, however, is not generally at equilibrium. Rather, its existence depends on the condition that mineral abundances, reactive surface areas, porosity and permeability vary slowly compared with the time required to form a stationary state. Such conditions are appropriate for geologic systems because the concentrations of aqueous species in a

representative elemental volume of the system are much less than their concentrations in coexisting minerals.

The concept of a stationary state is illustrated schematically in Fig. 1, where it is assumed that a porous rock column consisting initially of K-feldspar and an equilibrated solution (a) begins to react with an infiltrating solution that is not at equilibrium with K-feldspar. The first packet of solution displaces the equilibrated fluid and leaves behind reaction zones of gibbsite (starting at location $I^{(1)}{}_{\pi 1}$ and ending at $I^{(2)}{}_{\pi 1}$) and kaolinite (starting at location $I^{(1)}{}_{\pi 2}$ and extending downstream)(b). The gibbsite zone is stationary, but the kaolinite zone grows with time. The second and subsequent packets of the infiltrating solution interact with K-feldspar in exactly the same way as the first packet (c). The location of the gibbsite zone and beginning of the kaolinite zone consequently do not change with time, and appear to be stationary as long as associated changes in the porosity, volume fractions of reacting minerals, surface area and permeability are insignificant. Eventually, however, K-feldspar dissolves completely at the column inlet. The next fluid packet is undersaturated with respect to gibbsite when it reaches the previously deposited gibbsite zone, causing this mineral to dissolve at the upstream position of the zone and to precipitate farther downstream (d). The initial stationary state of the system (Fig.1, b-c) is in this way transformed into a new stationary state (Fig. 1,d).

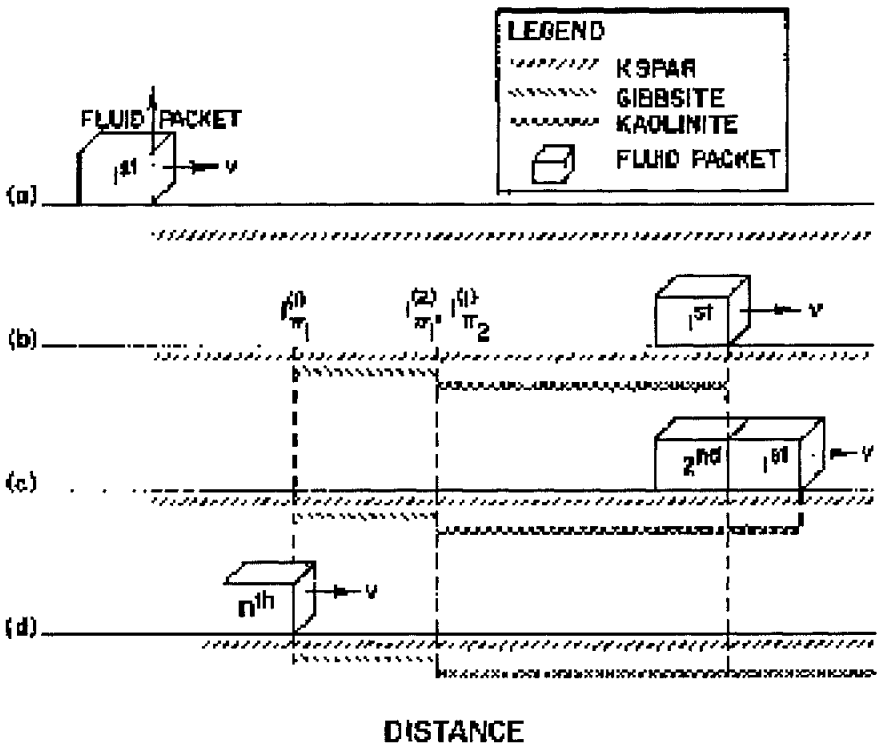

Figure 1: Schematic diagram illustrating the concept of stationary-states of an advective flow system resulting from coupled fluid flow and water-rock interaction (from Lichtner, 1988).

The mathematical formulation of the stationary-state approximation is straightforward when a Lagrangian reference frame is adopted (*i.e.*, fixed with respect to a reference mass or volume of fluid), and if constant one-dimensional advective fluid flow through

a homogeneous porous medium is assumed. Under such conditions a stationary state is represented by a set of first-order ordinary differential equations (Lichtner, 1988):

$$v\frac{d\psi_k}{dx} = -\sum_r \nu_{k,r}\frac{\partial \xi_r}{\partial t}(x;\phi_r), \tag{18}$$

where v stands for the Darcy fluid velocity, ψ_k (defined below) refers to the generalized concentration of the k-th *primary* species, x denotes the distance along the flow path, $\nu_{k,r}$ represents a stoichiometric coefficient for the k-th species in the r-th reaction involving dissolution of a mineral reacting at rate $\partial \xi_r / \partial t$, and ϕ_r stands for the mineral's volume fraction per unit volume of the porous medium. The generalized concentration is defined at a given position in the flow path and time t by:

$$\psi_k = C_k + \sum_i \nu_{k,i} C_i, \tag{19}$$

where C stands for the concentration of the subscripted aqueous species per unit volume of the liquid phase, and $\nu_{k,i}$ denotes a stoichiometric coefficient for the i-th *secondary* species formed with concentration C_i in a reaction involving destruction of the k-th primary species.

The reaction rate refers to dissolution of the r-th mineral. Assuming a general rate law for such reactions consistent with surface reaction control and transition state theory, it is given by (*e.g.*, Murphy and Helgeson, 1989):

$$\frac{\partial \xi_r}{\partial t} = \frac{\partial n_r}{\partial t} = -k_r s_r a_{H^+}^{\omega_{H^+}} \left[1 - \exp\left(-A_r / \sigma RT\right)\right], \tag{20}$$

where n_r represents the number of moles of the r-th mineral per unit volume of the porous medium, k_r stands for the rate constant for the corresponding reaction in which the mineral is a reactant, s_r refers to the total surface area per unit volume of the porous medium, ω_{H+} denotes the order of the reaction with respect to the activity of the hydrogen ion, A_r represents the chemical affinity for the overall reaction, σ stands for the ratio of the rate of decomposition of the activated complex to that of the overall reaction (normally taken as being equal to unity), R refers to the gas constant and T denotes temperature. The chemical affinity is given by:

$$A_r = RT \ln\left(K_r / Q_r\right), \tag{21}$$

where Q_r stands for the activity product. Assuming $\sigma = 1$, Eqn. (20) can be rewritten as:

$$\frac{\partial \xi_r}{\partial t} = -k_r s_r a_{H^+}^{\omega_{H^+}} \left(1 - \frac{Q_r}{K_r}\right), \tag{22}$$

where the logarithm of the quantity Q_r / K_r represents the saturation index. Thus, when $Q_r < K_r$, the reaction involves dissolution and the reaction rate is negative. For dissolution under far-from-equilibrium conditions, when $Q_r << K_r$, the reaction rate is given to a good approximation by:

$$\frac{\partial \xi_r}{\partial t} = -k_r s_r a_{H^+}^{\omega_{H^+}}, \tag{23}$$

and, for the special case $\omega_{H+} = 0$, this equation reduces to a linear rate equation that is independent of solution composition. When $Q_r > K_r$, the reaction involves precipitation and the reaction rate is positive. Equilibrium corresponds to the condition $Q_r = K_r$, in which case the overall reaction rate is equal to zero.

Hydrodynamic conditions control the amount of time a fluid packet is in contact with the minerals it encounters along a flow path. This time, referred to as the *residence* time and designated t', is related to distance along the flow path by (Lichtner, 1988);

$$dt' = \frac{\phi}{v} dx, \tag{24}$$

or, for conditions of constant porosity and Darcy flow velocity, by the integrated form;

$$t' = \frac{\phi x}{v}, \tag{25}$$

where ϕ refers to porosity. Equation (24) permits t' to be introduced as the independent variable in Eqn. (18):

$$\phi \frac{d\psi_k}{dt'} = -\sum_r \nu_{k,r} \frac{\partial \xi_r}{\partial t}(t';\phi_r), \tag{26}$$

which relates incremental changes in ψ_k to the rates of all mineral dissolution and precipitation reactions in which k participates as a reactant or product.

Equations (25) and (26) represent the Lagrangian formulation of the stationary-state approximation (Lichtner, 1988). Equation (25) constitutes the equation of motion for the center of mass of a fluid packet, whose chemical composition is determined by reactions, in accordance with Eqn. (26), by the residence time of the fluid in contact with the reacting minerals it encounters along the flow path. Minerals that precipitate as a result of water-rock interaction are left behind, and do not back react.

2.5.2 Chemical buffering in groundwater systems

A solution of Eqn. (26) for all primary aqueous species represents a reaction-path model of coupled fluid flow and water-rock interaction appropriate for advection-dominated groundwater systems (Lichtner, 1988). Kinetic constraints on the chemical buffering properties of these systems must therefore be compatible with mass-balance, charge-balance and mass-action constraints considered in the reaction path model.

To see this more clearly, we first transform Eqn. (26) into an equivalent expression written in terms of molalities rather than concentrations per unit volume of the aqueous phase:

$$\psi_k = \rho\left(m_k + \sum_i \nu_{k,i} m_i\right), \tag{27}$$

where ρ stands for the mass of the solvent, H_2O, per unit volume of the solution (given to a good approximation by the density of dilute solutions). Equation (26) can then be rewritten as:

$$\frac{d\psi_k}{dt'} = \rho\left(\frac{dm_k}{dt'} + \sum_i \nu_{k,i}\frac{dm_i}{dt'}\right) = -\frac{1}{\phi}\sum_r \nu_{k,r}\frac{\partial \xi_r}{\partial t}(t';\phi_r), \tag{28}$$

from which the change in molality of the k-th aqueous species is given by:

$$\frac{dm_k}{dt'} = -\frac{1}{\phi\rho}\sum_r \nu_{k,r}\frac{\partial \xi_r}{\partial t}(t';\phi_r) - \sum_i \nu_{k,i}\frac{dm_i}{dt'}. \tag{29}$$

Next, to provide a common basis for comparison of kinetic constraints imposed by Eqn. (29) with mass-balance, charge-balance and mass-action constraints described in preceding sections, we note that time-dependent variations in the overall reaction-progress variable are given by (*e.g.*, Wolery, 1992):

$$\frac{d\xi}{dt'} = \sum_r \frac{\partial \xi_r}{\partial t}(t';\phi_r). \tag{30}$$

Dividing both sides of Eqn. (29) by $d\xi/dt'$ results in:

$$\frac{dm_k}{d\xi} = -\frac{1}{\phi\rho}\sum_r \nu_{k,r}\frac{d\xi_r}{d\xi} - \sum_i \nu_{k,i}\frac{dm_i}{d\xi}, \tag{31}$$

where the "fractional rate", $d\xi_r/d\xi$ (Wolery, 1992), is given by:

$$\frac{d\xi_r}{d\xi} = \frac{\frac{\partial \xi_r}{\partial t}(t';\phi_r)}{\sum_r \frac{\partial \xi_r}{\partial t}(t';\phi_r)}. \tag{32}$$

Equation (31) indicates that the fractional rates of mineral dissolution and precipitation reactions involving the k-th primary species as a reactant or product will control the net flux of that species into or out of the fluid packet. Additional changes in the molality of the k-th species may come from aqueous dissociation reactions forming the i-th secondary species. If, as here, it is assumed that the aqueous reactions are sufficiently fast to sustain equilibrium, kinetic constraints on the chemical buffering properties of the system are controlled solely by the flux term. The coupling between hydrodynamics and reaction kinetics arises from the dependence of the reaction rate on the residence time (t'), which at a given location in the flow path is determined by the fluid-flow velocity and porosity [Eqn. (25)]. Kinetic constraints on the chemical buffering properties of groundwater systems under stationary-state conditions are imposed by Eqn. (31), because this equation partially controls the value of the derivative, $dm_k/d\xi$, appearing in Eqn. (5).

Although the stationary-state model is useful for conceptualizing kinetic controls on the chemical buffering properties of groundwater systems, it should be emphasized that the model is based on a highly idealized representation of such systems. Model conditions of pure advective flow in a homogeneous porous medium may not occur in real groundwater systems, except over extremely limited scales of space and time. It should also be noted that mineral weathering rates deduced from field observations of natural systems have been found to be slower by several orders of magnitude than rates calculated using the theoretical concepts of mineral-fluid reaction kinetics discussed above (*e.g.,* Drever and Clow, 1994). With these limitations and uncertainties in mind, the stationary-state model nevertheless provides a useful conceptual framework for describing general kinetic controls on the chemical buffering properties of natural systems resulting from the coupled processes of fluid flow and water-rock interaction.

2.6 Summary

The chemical buffering properties of multicomponent, multiphase systems are conditional properties in the sense that they refer to a specific aqueous species in a system that is open with respect to a specific reactant. A mathematical statement of this concept in terms of parameters considered in the reaction-path model is given by Eqn. (2). A solution of this equation requires evaluation of the dependence of the activity of the buffered species on incremental changes in the overall reaction-progress variable. This dependence is represented by a truncated Taylor's series expansion [Eqn. (5)], where the values of associated derivatives are estimated using finite-difference techniques and mass-balance, charge-balance and mass-action constraints given by Eqns. (8), (12) and (17), respectively. Kinetic constraints on buffering behavior can be described if the relation between reactant flux and reaction rate is well defined. This relation is explicit for the important case of advective groundwater flow and water-rock interaction, where kinetic constraints on the chemical buffering properties of groundwater systems under stationary-state conditions are represented by Eqn. (31).

In practice, charge-balance and mass-action constraints represented by Eqns. (12) and (17) are substituted for relevant terms appearing in mass-balance equations [Eqn. (8)]. This simplifies the computational procedure necessary to solve a reaction-path model by condensing the "grand matrix equation" (Helgeson *et al.*, 1970; Wolery, 1992) representing reversible mass transfer and conservation of mass and charge among all the phases and components in the system of interest. The reaction-path model and associated numerical-solution techniques are incorporated in several software packages, including EQ3/6 (Wolery, 1992) and the Geochemist's Workbench (GWB; Bethke, 1996). These codes are used in the following section to estimate the buffering properties of natural systems and engineered barriers, and to estimate associated attenuation factors limiting the migration velocity of reaction fronts.

3 Attenuation of reaction-front migration by chemical buffering

In this section we apply the concept of chemical buffering to processes that could affect the performance of a deep geologic repository for nuclear waste. Specifically, we build upon the suggestion by Rosing (1993) that an inverse relation must exist between the buffer intensity, β, and the migration velocity of reaction fronts in systems involving advective or diffusive mass transport. Effective buffering (*i.e.*, where associated values of β are relatively large) should therefore tend to minimize the rate at which a chemical signal, or perturbation, propagates through a repository's system of natural and engineered barriers. A quantitative understanding of this apparent relation between buffer intensity and front migration could provide a basis for evaluating the potential role of chemical buffering in achieving the isolation and retardation functions of the EBS and geosphere that were noted in the introduction.

Mathematical statements of this relation are derived in Sections 3.1 and 3.2 specifically for the case of a pH front migrating through the KBS-3 buffer and a granitic host rock, respectively. The front is taken to represent a boundary separating two regions of the buffer or granite where the concentration of H^+ differs significantly. We consider pH because this parameter is determined by a large number of homogeneous and heterogeneous reactions, and because pH is an important determinant of the stability of EBS materials and of radioelement speciation, sorption and solubility behavior. The basic approach is general, however, and can be extended to other parameters, such as the redox potential, which are also important determinants of repository performance, and which are subject to chemical buffering control of reaction-front migration.

3.1 Attenuation of reaction fronts in the buffer

The effects of chemical buffering on the migration of a pH front through the KBS-3 buffer are evaluated in this section. A conceptual model of the relevant processes is shown in Fig. 2, which represents the KBS-3 EBS in terms of a radial coordinate system with transport in the r-direction. We assume that the initial pH of groundwater in the host rock is 6, and that the initial pH of buffer porewaters is 9. The gradient in H^+ concentration causes hydrogen ions to diffuse into the buffer. Resultant changes in pH stimulate aqueous-speciation reactions and other, heterogeneous reactions among the minerals in the buffer. Associated effects on pH buffering properties are assumed to be represented by the buffer intensity, β (modified as noted below), which is equivalent to the inverse of the buffer sensitivity given by Eqn. (1) [see Section 2]. This assumption implies that the region of the pH front corresponds to a closed chemical system, and that all reactions equilibrate over a period of time that is short relative to the flux of H^+ into this system. Although the validity of this assumption may be questionable, the following analysis should approximate the effects of chemical buffering on front migration under limiting conditions of local equilibrium.

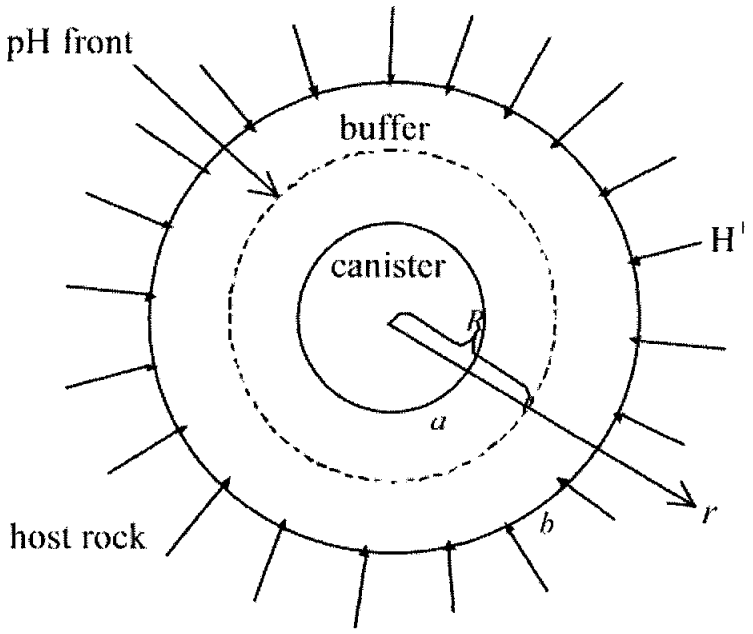

Figure 2: Conceptual model of the migration of a pH front (dashed line) through the buffer. The inner and outer radii of the buffer are labeled a and b, respectively.

3.1.1 Model description

The spatial and temporal concentration distribution of H^+ in the buffer (Fig. 2) is governed by the following equations:

$$\frac{\partial C}{\partial t} + D\left(\frac{\partial^2 C}{\partial r^2} + \frac{1}{r}\frac{\partial C}{\partial r}\right) = 0, \qquad a \le r \le b, \quad t > 0, \tag{33}$$

with initial and boundary conditions given by,

$$C(r,0) = C_0 \tag{34a}$$

$$C(b,t) = C_1, \quad \text{and} \quad C(R,t) = C_0 \quad \text{if} \quad a < R(t) < b \tag{34b}$$

$$C(b,t) = C_1 \quad \text{and} \quad \left.\frac{\partial C}{\partial r}\right|_{r=a} = 0 \quad \text{if} \quad R(t) = a \tag{34c}$$

$$-D\phi\left.\frac{\partial C}{\partial r}\right|_{r=R} = \beta'\frac{dR}{dt}, \qquad t > 0. \tag{35}$$

and,

$$R(0) = b. \tag{36}$$

The unknown variable, C, refers to the hydrogen ion concentration (mol l^{-1}), C_1 and C_0 represent the initial concentration in the host rock and buffer, respectively, D stands for the diffusion coefficient [$cm^2\ s^{-1}$], ϕ denotes porosity, and β' refers to the *total* pH buffer intensity (meq l^{-1}). The total buffer intensity is given by:

$\beta' = \beta \times \Delta pH$,

and is used here in place of the buffer intensity defined by the inverse of Eqn. (1) as a matter of convenience. Equation (33) describes the transport of H^+ from the host rock into the buffer. Equation (35) represents a mass balance at the location R (Fig. 2), marking the position of the pH front. This location delimits a region in the buffer, given by $R \leq r \leq b$, within which the pH buffer intensity has been exhausted. Coupled Eqns. (33) and (35) fix the location of the pH front until the cumulative diffusive flux of H^+ into the front is equal to the buffer intensity, at which time the front migrates toward the canister.

Equations (33) – (36) represent a type of moving-boundary problem that is frequently encountered in studies of heat and mass transfer involving a change in phase (*e.g.*, Eckert and Drake 1972). Although an exact solution of such problems is difficult to obtain, two solution techniques provide close approximations to the exact solution: (1) a simplified analytical technique, and (2) an adaptive-grid numerical technique. Application of these solution methods is described in Sections 3.1.3 and 3.1.4, respectively. Before proceeding to a discussion of these solutions, however, values for the parameter β'must first be estimated, and this task is therefore taken up in the following section.

3.1.2 Estimation of the pH buffer intensity of MX-80 bentonite

To estimate values of β'appearing in Eqn. (35), we use the EQ3/6 geochemical software package (Wolery, 1992) and a modeling approach described by Roaldset *et al.* (1996) to simulate an experimental acid-base titration of water-saturated MX-80 bentonite (which may be used as the buffer material in the KBS-3 EBS). The first step in the simulation is to equilibrate the bentonite (30% porosity) with a reducing granitic groundwater at 15°C and pH 8.1. The bentonite is assumed to consist initially of smectite (75%), quartz (15%), plagioclase (5%), pyrite (3%), and calcite (2%). Smectite is assumed to be an ideal solid solution of Na-, K-, Ca-, and Mg-montmorillonite, -nontronite, and beidellite end members, initially with 69 mol% Na-montmorillonite, 23 mol% Ca-montmorillonite, 6 mol% Mg-montmorillonite, 1 mol% K montmorillonite, and 0.125 mol% each of the other components. Model results indicate that following initial equilibration of bentonite with the groundwater, plagioclase is converted to a clinoptilolite solid solution enriched in Na and Ca, and smectite is slightly enriched in the montmorillonite end members at the expense of the nontronite and beidellite end members. The calculated pH of the equilibrated porewater is 8.4.

An acid-base titration of the equilibrated bentonite-porewater system is then simulated by modeling the incremental addition of small quantities of a strong acid or strong base to the system, and calculating resultant changes in pH. Local and partial equilibrium are assumed, and results are used to generate a titration curve depicting changes in pH versus the number of moles of strong acid or strong base added to the system. The pH buffer intensity is then calculated from the inverse slope of the titration curve. The buffer intensity and buffer capacity are related to specific reactions by monitoring calculated variations in the masses of reactant and product minerals.

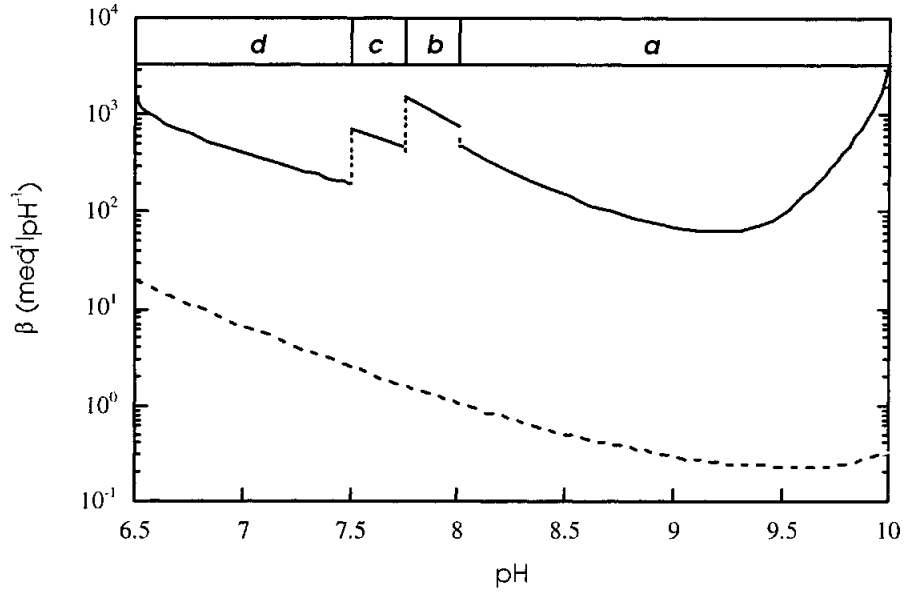

Figure 3: Calculated pH buffer intensities of MX-80 bentonite (solid line) and calcite (long-dashed line). Vertical short-dashed lines indicate discontinuities in buffering behavior resulting from exhaustion of the buffer capacity of mineral assemblages a, b and c (see text).

Results of the titration simulation are shown as a function of pH in Fig. 3, where it can be seen that four mineral assemblages control buffering behavior. The mineralogy of the buffer assemblages (pH regions *a* - *d*, Figure 3) are:

a- smectite (↓), clinoptilolite (↓), quartz (↑),

b- smectite (↑), clinoptilolite (↓), quartz (↓), scolecite (↑),

c- smectite (↑), clinoptilolite (↓), quartz (↑), scolecite (↑), kaolinite (↑), and

d- smectite (↓), quartz (↑), scolecite (↓), kaolinite (↑),

where the symbols, ↑and ↓, denote increasing and decreasing mass, respectively, with decreasing pH. The transition between buffer assemblages is characterized by initial precipitation and/or complete dissolution of one or more minerals. For example, the transition from assemblage *b* to *c* is initiated by kaolinite precipitation. Clinoptilolite dissolves with further reduction in pH, and assemblage *d* evolves from assemblage *c* when clinoptilolite's mass is exhausted. The buffer capacity in this sequence is therefore determined by the masses of kaolinite and clinoptilolite. The corresponding buffer intensities for these assemblages also differ significantly, and these differences together with the limited buffer capacities of kaolinite and clinoptilolite generate sharp discontinuities in the overall buffering behavior.

For comparison, the calculated buffer intensity of calcite is also plotted in Fig. 3. Although calcite is often assumed to exert a strong control on the pH of bentonite porewaters, it can be seen that the buffer intensity of calcite is small compared to that of the clay minerals, quartz, and zeolites. This supports the conclusion that heterogeneous equilibria among aluminosilicate minerals should provide more resistance to pH changes than do reactions involving carbonate minerals, ion-exchange reactions, or

homogeneous reactions involving weak acids or bases (Hutcheon *et al.*, 1993; Stumm and Morgan, 1996). The latter reactions are generally much faster than the former (Kittrick, 1979), which suggests that they may control the pH buffering properties of bentonite over relatively short periods of time. The longer term pH buffering properties of bentonite may be controlled, however, by reactions involving the smectite clays and other aluminosilicate minerals.

Based on the results shown in Fig. 3, we estimate a range of values for β' [*i.e.*, = 3 x β, see Section 3.1.1] roughly between 1 and 1000 meq l^{-1}. The latter value may be a reasonable estimate for MX-80 bentonite if equilibrium is rapidly achieved among all mineral-porewater reactions. The former value may be more realistic if only calcite equilibrates, *i.e.*, if reactions involving the smectite clays and other aluminosilicate minerals are too slow to equilibrate with H^+ diffusing into the pH front. The selected range in values of the total buffer intensity is intended to bound these two possibilities.

3.1.3 Analytical solution

This solution technique is based on the assumption that the migration of the pH front is slow compared to the diffusive transport of H^+. This assumption may be valid if the total buffer intensity is strong (*e.g.*, if $\beta' > 1$). In such cases, a steady-state concentration profile may be assumed for H^+ behind the front:

$$C(r,t) = C_1 - (C_1 - C_0)\frac{\ln r/b}{\ln R(t)/b}, \quad R(t) \le r \le b. \tag{37}$$

and it is then unnecessary to solve the coupled system of Eqns. (33) – (36). Substitution of Eqn. (37) into Eqn. (35) results in:

$$x \ln x \frac{dx}{d\tau} = \frac{\Delta C}{\beta'} \quad \text{with} \quad x(0) = 1. \tag{38}$$

where $x = \frac{R(t)}{b}$, $\tau = \frac{D\phi t}{b^2}$, and $\Delta C = C_1 - C_0$.

A solution of Eqn. (38) is given by:

$$\frac{\Delta C}{\beta'}\tau = x^2\left(\frac{1}{2}\ln x - \frac{1}{4}\right) + \frac{1}{4}. \tag{39}$$

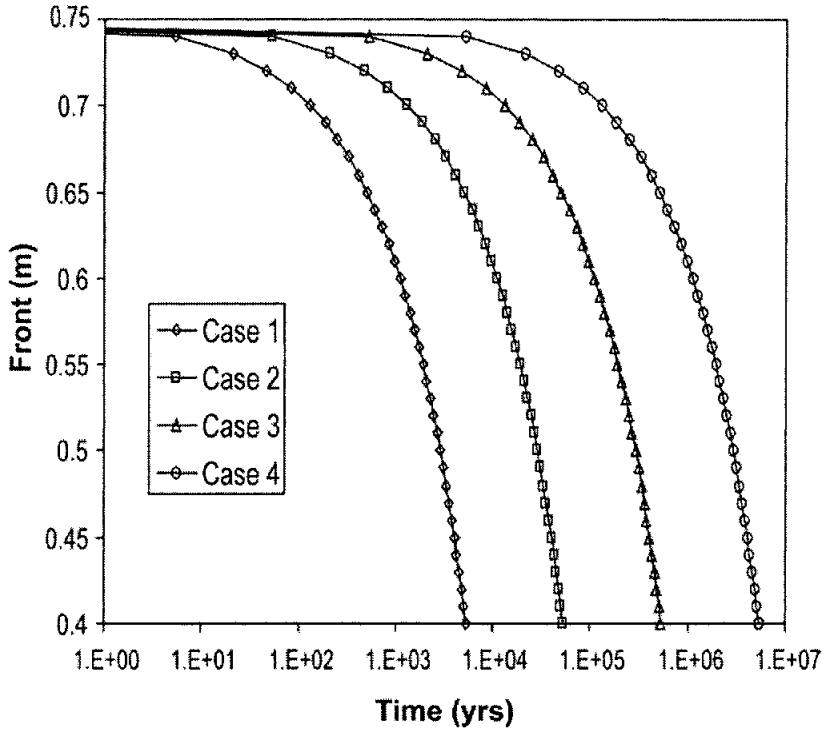

Figure 4: pH front migration calculated using the analytical model. Case 1: $\beta' = 1$ meq l^{-1}; Case 2: $\beta' = 10$ meq l^{-1}; Case 3: $\beta' = 100$ meq l^{-1}; Case 4: $\beta' = 1000$ meq l^{-1}.

Results are shown in Fig. 4 for the assumed range in values of the total buffer intensity estimated in Section 3.1.2, and assuming $D = 10^{-5}$ cm^2 s^{-1}, $\phi = 0.3$, a and $b = 0.4$ m and 0.75 m (see Fig. 2), respectively, and initial H^+ concentrations in the host rock and buffer = 10^{-6} mol/l and 10^{-9} mol/l, respectively (*i.e.*, $\Delta C \approx 10^{-3}$ meq l^{-1}). As can be seen, the estimated time for the front to arrive at the buffer-canister boundary varies between 5.3×10^3 years ($\beta' = 1$ meq l^{-1}) to 5.3×10^6 years ($\beta' = 1000$ meq l^{-1}). This time, denoted t_f (year), is readily calculated using Eqn. (39) and the substitution $x = a/b$:

$$t_f = 5.31 \frac{\beta'}{\Delta C}. \tag{40}$$

Equation (40) indicates that for a given value of ΔC the time for the front to reach the bentonite-canister boundary is proportional to the total buffer intensity. Thus, as the intensity of pH buffering increases, the migration velocity of the pH front decreases

It is important to note that methods for obtaining simplified analytical solutions to moving-boundary problems are not unique (Eckert and Drake 1972; P. Robinson 1998). The approach used here is appropriate and reasonably accurate, however, as demonstrated in the following section.

3.1.4 Numerical solution using adaptive grids

This solution technique uses a fully implicit finite-difference technique, and an object-oriented programming approach and associated solver to solve Eqns. (33) to (36). The solver, PETSc (Programmable Extensible Toolkit for Scientific computations) is described by Balay *et al.* (1997), and is available from Argonne National Laboratory.

The computations simulate the movement of a pH front in the EBS buffer starting at a time that is estimated from the finite-difference form of Eqn. (35)

$$t_{start} = \frac{\beta'}{D\phi}\frac{\Delta R^2}{C_1 - C_0} \tag{41}$$

Initially, a small number of grids are employed for the region between the buffer-host rock interface and the front in order to calculate spatial variations in H^+ concentration. At each timestep, after concentrations at all nodal points are obtained, the amount of H^+ transferred into the front is calculated. The new front position is then calculated using the finite-difference form of Eqn (35). The number of grids is increased for the new front position up to a specified maximum number. Upon increasing the number of grids, the concentration profile for the next step in the computation is calculated by estimating the current concentration profile over the new gridding system using an interpolation technique. At each timestep, global and local mass balance errors are checked and are used to adjust the size of the time steps to minimize errors.

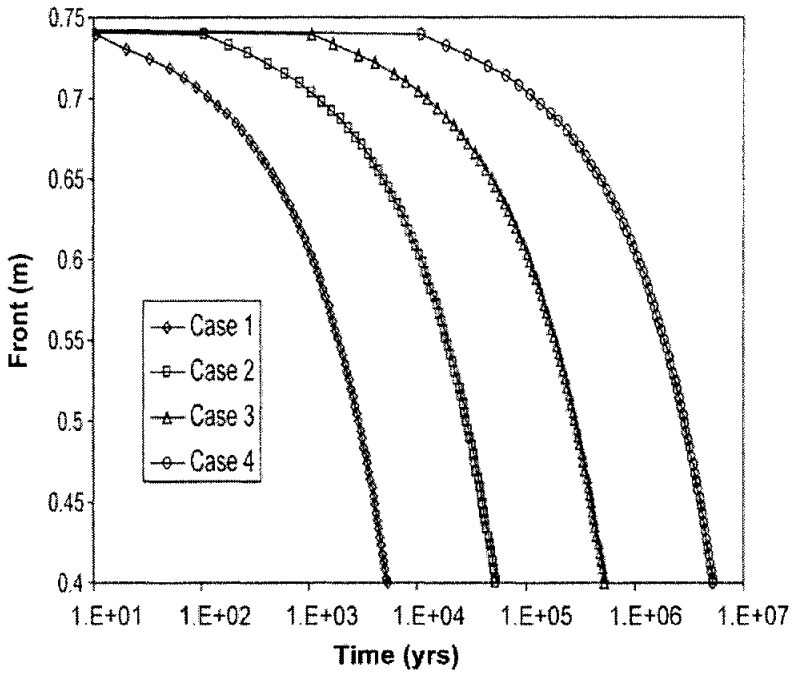

Figure 5: pH front migration calculated using the adaptive-grid numerical model. Case 1: $\beta' = 1$ meq l^{-1}; Case 2: $\beta' = 10$ meq l^{-1}; Case 3: $\beta' = 100$ meq l^{-1}; Case 4: $\beta' = 1000$ meq l^{-1}.

Results of the pH-front migration simulation using the adaptive-grid procedure are shown in Fig. 5. Parameter values used to constrain the adaptive-grid calculations are identical to those used in the analytical model (Section 3.1.3). As can be seen, the

calculated time for the front to reach the bentonite-canister boundary varies from 5.3×10^3 to 5.3×10^6 years, depending on the value assumed for β'. This time, t_f (Section 3.1.3), is given to a good approximation by:

$$t_f \approx 5.29 \frac{\beta'}{\Delta C}, \tag{42}$$

which is nearly identical to the equation for t_f derived from the analytical model [Eqn. (40)]. It should be noted that after the front first arrives at the buffer-canister boundary, the pH of the bentonite porewater continues to slowly increase, as a consequence of molecular diffusion, until the concentration within the bentonite becomes uniform and equal to that of the host rock. This steady state is achieved 50 to 90 years after the front first arrives at the boundary.

pH profiles are plotted in Figs. 6 and 7 at several front positions and times for Case 1 (β'= 1 meq l^{-1}) and Case 4 (β'= 1000 meq l^{-1}), respectively. Comparison of the figures indicates that the concentration profiles for a given front location are identical, but are established at different times. This is because the governing Eqns. (33) and (34) are not constrained by the total buffer intensity. This parameter only affects the front position, as determined by Eqn. (35). The concentration of H^+ at the front will not increase until the buffer intensity is exceeded by the cumulative flux of H^+ to the front.

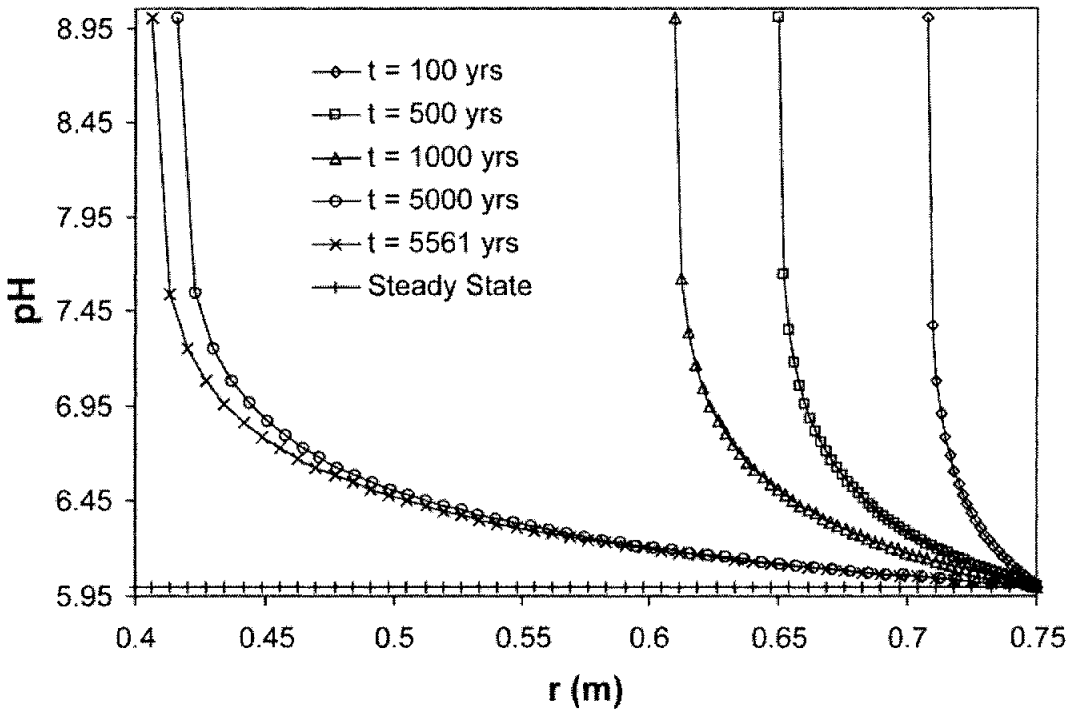

Figure 6: pH profiles at different times and front positions in the buffer for Case 1 (β' = 1 meq l^{-1}).

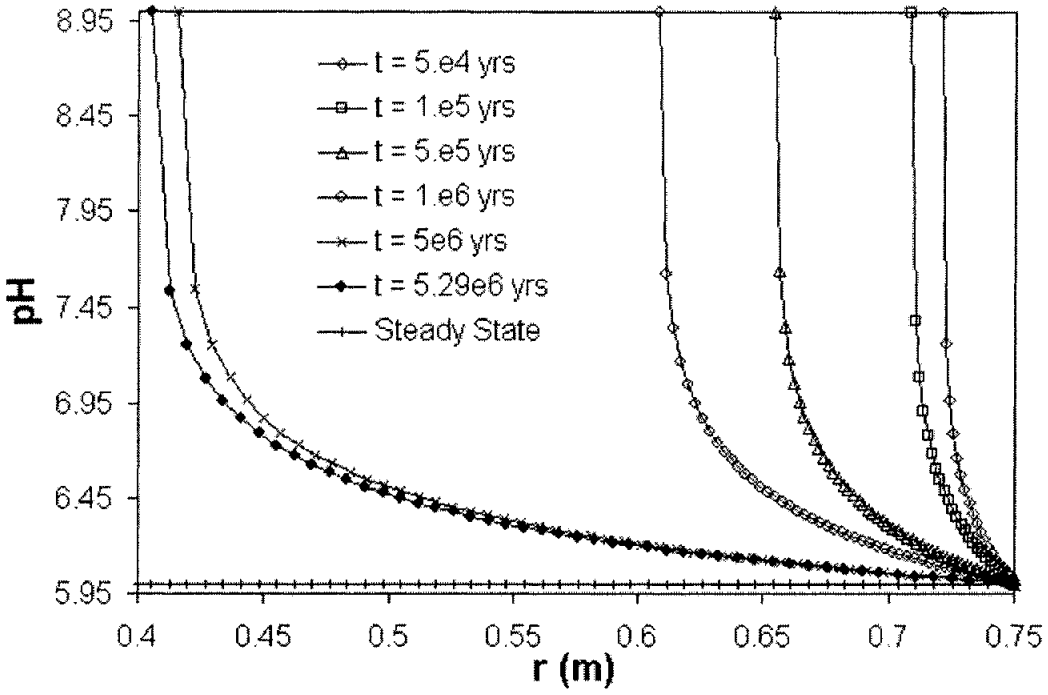

Figure 7: pH profiles at different times and front positions in the buffer for Case 4 ($\beta' = 1000$ meq l^{-1}).

Calculated front positions using the analytical and adaptive grid models are plotted in Fig. 8. As can be seen, front positions calculated using these two modeling approaches are nearly identical.

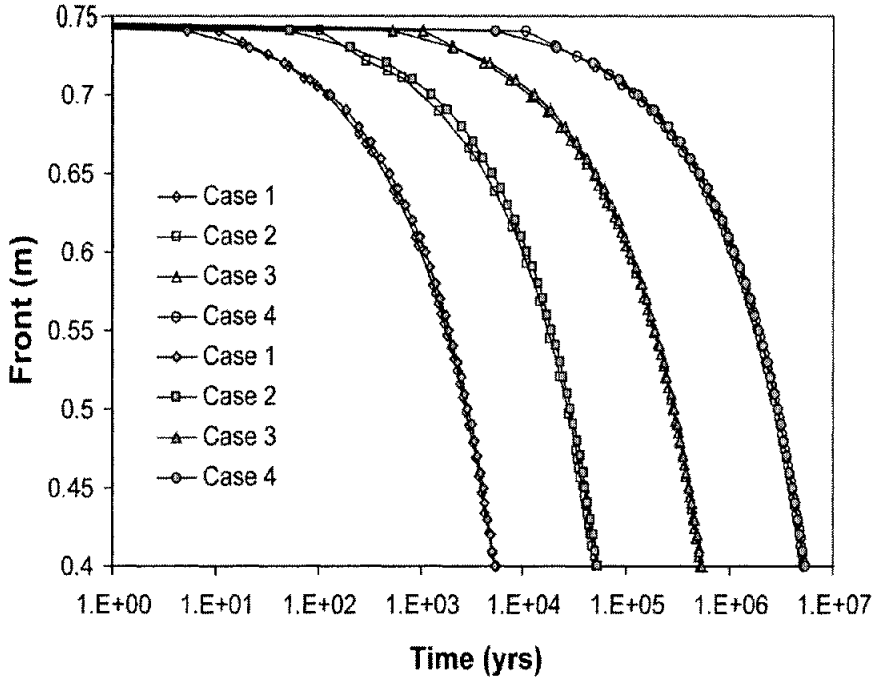

Figure 8: Comparison of pH front migration calculated using the analytical model (gray symbols) and adaptive-grid numerical model (open symbols) [cases 1 – 4 for the analytical and adaptive-grid models are as defined in the captions to Figs. 4 and 5, respectively.

3.1.5 Comparison of analytical and numerical results

The analytical and adaptive-grid numerical solutions to Eqns. (33) – (36) produce results that are nearly identical. Differences in calculated values amount to less 0.6%, as demonstrated by the comparison shown in Fig. 9.

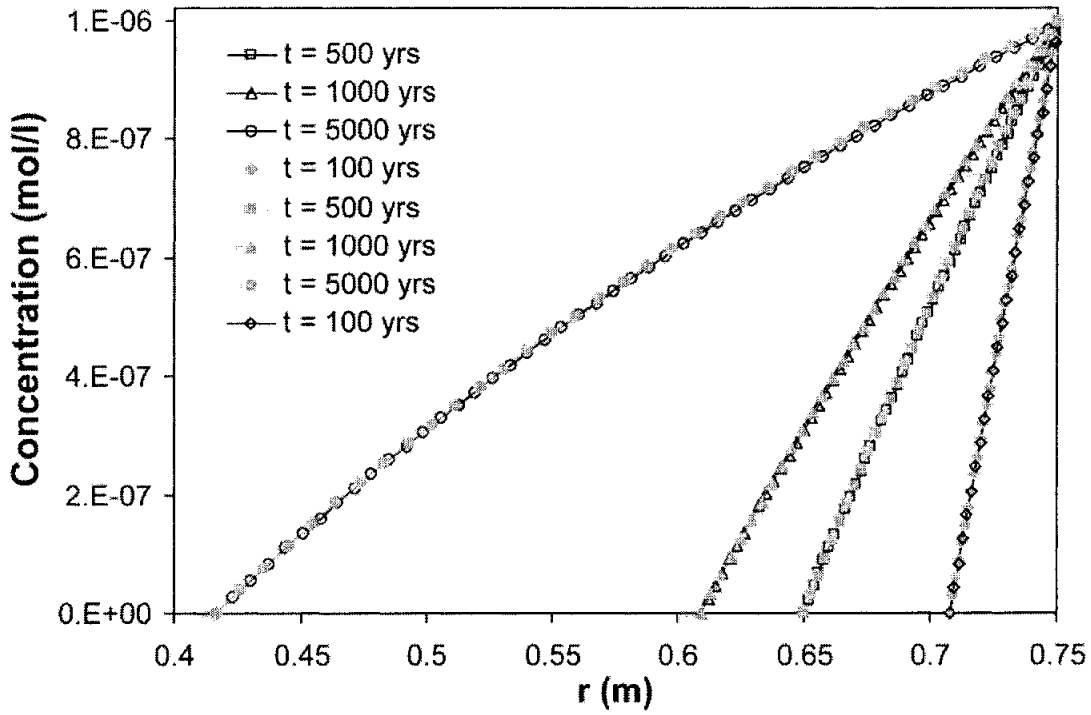

Figure 9: Comparison of hydrogen-ion concentrations calculated using the analytical model (gray symbols) and adaptive-grid numerical model (open symbols) [cases 1 – 4 for the analytical and adaptive-grid models are as defined in the captions to Figs 4 and 5, respectively.

This appears to justify our assumption in deriving the analytical solution, *i.e.*, that a steady-state concentration profile will exist behind the front. Such quasi steady-state behavior is also predicted by the numerical model, where the maximum difference between "current" and "previous" solutions is found to be extremely small. Hence, the simplified solution represented by Eqns. (39) or (40) can be used for a quick and accurate evaluation of pH front migration in the buffer. It should be emphasized, however, that these conclusions may not be valid if the total buffer intensity is smaller than assumed here (*e.g.*, < 1 meq l^{-1}).

3.1.6 Summary

Two solution methods are developed for simulating the migration of a pH front through the KBS-3 buffer: a simplified analytical method and an adaptive grid numerical technique. For the parameters considered here, the time for the pH-front to reach the bentonite-canister boundary varies from about 5,000 to 5,000,000 years. The most rapid arrival time corresponds to the weakest buffering (assuming that only calcite equilibrates with bentonite porewaters). The latest arrival time corresponds to the

strongest buffering (equilibration of all bentonite minerals with buffer porewaters). Steady-state concentration profiles prevail behind the front. The two solutions are essentially equivalent, indicating that the simplified analytical solution is appropriate for this type of problem. Two assumptions that are adopted provisionally in both models may be require additional consideration, however - 1) that the region near the pH front is a closed chemical system, and 2) that local and partial equilibrium is sustained as H^+ diffuses into this region. Moreover, the solutions derived in this study may only be valid for values of β' greater than about 1 meq l^{-1}.

3.2 Attenuation of reaction fronts in geologic systems

Lichtner (1988) notes that reaction-front velocities under stationary-state conditions (Section 2.5.1) are attenuated relative to the Darcy flow velocity by an amount that is inversely proportional to a "retardation factor". We follow Lichtner's derivation of this relation in the following section to determine whether such retardation factors can be interpreted in terms of the chemical buffering properties of reactions controlling front migration. If so, such behavior may be consistent with the suggestion by Rosing (1993) that front velocities must be inversely proportional to the buffer intensity. A geochemical modeling approach compatible with the stationary-state model is then used to estimate retardation factors limiting the migration velocity of a pH front in granitic host rocks.

3.2.1 Model description

Lichtner's derivation is based on a continuum representation of mass transport in a porous medium involving a multicomponent system of reacting minerals and fluid (Lichtner, 1988). Homogeneous reactions among aqueous species are assumed to be sufficiently fast to sustain equilibrium. Heterogeneous reactions among minerals and the aqueous phase are, however, described in terms of kinetic rate laws, for which local equilibrium is a limiting case. Reactions involving primary aqueous species, j, and irreversibly reacting minerals, r, are represented by the following set of $N + M$ coupled, non-linear partial differential equations:

$$\frac{\partial}{\partial t}\left(\phi\psi_j\right) + \nabla\cdot\Omega_j = -\sum_{r=1}^{M} \nu_{j,r}\frac{\partial\xi_r}{\partial t}\ (j = 1,...,N), \text{ and} \tag{43}$$

$$\frac{\partial}{\partial t}\left(\phi_r V_r^{-1}\right) = \frac{\partial\xi_r}{\partial t}\ (r = 1,...,m). \tag{44}$$

Equations (43) and (44) refer to aqueous species and minerals, respectively. The parameter V_r denotes molar volume and Ω_j represents the generalized flux (see Lichtner (1988) for further discussion of the flux term; other symbols are as defined in Section 2.5.1). Lichtner (1988) combines Equations (43) and (44) to obtain the transient mass conservation equations for a single spatial dimension:

$$\frac{\partial}{\partial t}\left(\phi\psi_j + \sum_{r=1}^{M} \nu_{j,r} V_r^{-1} \phi_r\right) - \phi D \frac{\partial^2 \psi_j}{\partial^2 x} + v \frac{\partial \psi_j}{\partial x} = 0 \tag{45}$$

where D refers to the diffusion coefficient matrix consisting of equal and constant elements for primary and secondary species containing j.

Lichtner (1988) next invokes the traveling wave approximation (Ortoleva *et al.*, 1986) to derive an expression for the velocity of a reaction front. The approximation is used to specify a coordinate system at rest with respect to a Lagrangian fluid packet moving with the front. This fluid packet is thus co-located with the front and moves at the same velocity. The approximation assumes that in the vicinity of a reaction front the solution to the mass-transport equations can be represented in the form of a traveling wave, given by:

$$\psi_j(x,t) = \psi_j(x - l(t)), \text{ and} \tag{46}$$

$$\phi_r(x,t) = \phi_r(x - l(t)), \tag{47}$$

for the generalized solute concentration and mineral volume fraction, respectively. It is assumed that one or more reaction fronts may exist, with the front of interest located at position $l(t)$, propagating with velocity $v_f = dl/dt$. Lichtner (1988) notes that Eqns. (46) and (47) are not valid when diffusional transport is important, and that the traveling wave approximation is therefore valid only for purely advective transport.

Adopting the traveling wave approximation permits transformation of Eqn. (45) to:

$$\frac{d}{dx'}\left\{-\phi D \frac{d\psi_j}{dx'} + v\psi_j - v_l\left(\phi\psi_j + \sum_{r=1}^{M} \nu_{j,r} V_r^{-1} \phi_r\right)\right\} = 0. \tag{48}$$

using the approximations for $\psi_j(x,t)$ and $\phi_r(x,t)$ given by Eqns. (46) and (47), respectively, with reference to the coordinate x', defined by

$$x' = x - l(t). \tag{49}$$

From Eqn. (48) it follows that:

$$-\phi D \frac{d\psi_j}{dx'} + v\psi_j - v_f\left(\phi\psi_j + \sum_{r=1}^{M} \nu_{j,r} V_r^{-1} \phi_r\right) = \text{constant}. \tag{50}$$

Evaluating the left-hand side of this equation at two distinct points, one upstream of the reaction front and the other downstream, yields the following expression for the front velocity for the case when the first term in the equation is negligible compared to the second and third terms (*i.e.*, for advective transport):

$$v_f = \frac{v}{\phi R}, \tag{51}$$

where the retardation factor, R, is given by:

$$R = 1 + L_j \cdot \tag{52}$$

with coefficient L_j given by:

$$L_j = \frac{\sum_{r=1}^{M} \nu_{j,r} V_r^{-1} \langle \phi_r \rangle}{\phi \langle \psi_j \rangle} \cdot \tag{53}$$

The brackets in Eqn. (53) refer to the difference in the enclosed quantity at the two chosen points.

Recalling that Eqn. (53) refers to a packet of fluid that is co-located with the reaction front, the coefficient L_j, and thus the retardation factor R, must depend on the buffer intensity. This is because changes in solution chemistry are then explicitly correlated with the flux of reactants into or out of the fluid packet as a result of those mineral-fluid reactions that define the front. The numerator in Eqn. (53) thus defines the cumulative flux of species j into or out of the fluid packet, and the denominator defines corresponding changes in the generalized concentration, ψ_j, of this species. For the limiting case where the generalized concentration refers to the activity of a single aqueous species, Eqn. (53) is identical to the buffer intensity given by the inverse of Eqn. (1). In the more general case, L_j represents the buffer intensity with respect to both primary and secondary species of j. In either case, Eqns. (51) to (53) indicate that the migration velocity of a reaction front will be attenuated by a retardation factor that is closely analogous, or identical, to the buffer intensity of reactions that define the front.

3.2.2 Estimation of attenuation parameters for a pH front in granite

As noted in Section 2.5.1, Eqns. (26) represent a conventional reaction-path model of water-rock interaction in an open system. Solution of these equations yields the concentrations of aqueous species and mineral reaction rates as a function of time. Taking this time to represent the residence time of a fluid packet traversing the system enables temporal variations in solution composition, mineralogy and mineral reaction rates to be calculated using Eqn. (25) as a function of location in the flowpath. This spatial transformation of the reaction-path data permits calculation of the attenuation parameter, L_j, using Eqn. (53).

To demonstrate this modeling approach with the specific objective of estimating attenuation parameters for a pH front in a granitic repository host rock we first calculate a reaction path simulating the alteration of a representative granite, consisting initially of K-feldspar and quartz, by an acidic (pH 4) infiltrating groundwater at 25°C [see also Lichtner (1988)]. The conceptual model for this system is similar to that illustrated in Fig. 1. The infiltrating solution is assumed to be out of equilibrium with respect to K-feldspar and quartz. As these minerals dissolve a sequence of alteration minerals precipitate in the order gibbsite - kaolinite – muscovite. The final solution is equilibrated with both muscovite and K-feldspar, and is supersaturated with respect to quartz due to its sluggish precipitation rate. The initial volume fractions of K-feldspar

and quartz are assumed to be 20 and 70%, respectively, and the corresponding surface areas are 12 and 40 $cm^2\ cm^{-3}_{rock}$. The solution migrates through the host rock (porosity = 10%) with a Darcy flow velocity of 10 m yr^{-1}.

To simulate the reaction path corresponding to this conceptual model we use the open-system, reaction-path model in the geochemical software package GWB (Bethke, 1996) and pH-independent apparent rate constants from Lichtner (1988) for hydrolysis reactions involving K-feldspar ($k = 10^{-15.5}$ mol cm^{-2} sec^{-1}) and quartz ($k = 10^{-17.5}$ mol cm^{-2} sec^{-1}). The surface areas for K-feldspar and quartz are converted to values consistent with Eqn. (20) in GWB ($cm^2\ l^{-1}$) by dividing by the porosity and multiplying by a conversion factor equal to 1000 $cm^3\ l^{-1}$. Resultant values are 120,000 $cm^2\ l^{-1}$and 400,000 $cm^2\ l^{-1}$, respectively. Local equilibrium conditions for gibbsite, kaolinite and muscovite are modeled by assuming that the corresponding precipitation rates are instantaneous.

The results of the simulation are shown by the bold curve on the *activity-activity* diagram for the K_2O-Al_2O_3-SiO_2-H_2O system in Fig. 10. The reaction path advances along this curve from the lower left to the upper right. Gibbsite begins to precipitate at local equilibrium and continues to precipitate as both K-feldspar and quartz dissolve. Resultant variations in solution compositions then evolve to conditions where both gibbsite and kaolinite precipitate (point *a*). Continued dissolution of K-feldspar and quartz extends the path into the kaolinite stability field, where gibbsite no longer precipitates. Quartz ceases to dissolve and begins to precipitate at the kinetically controlled rate when $\log a_{SiO2(aq)} > -3.99$ (point *b*), near which point the reaction path takes an upward track and approaches local equilibrium of the aqueous phase with respect to both kaolinite and muscovite (point *c*). Continued dissolution of K-feldspar and precipitation of quartz extends the path into the stability field of muscovite, and it then approaches the stability boundary between muscovite and K-feldspar (point *d*). The path parallels this boundary as K-feldspar continues to dissolve at an extremely low, close-to-equilibrium rate, and quartz continues to slowly precipitate. At the final stage of the reaction path *(e)*, K-feldspar is effectively equilibrated with the aqueous phase, as is muscovite, and the solution is very slightly supersaturated with respect to quartz.

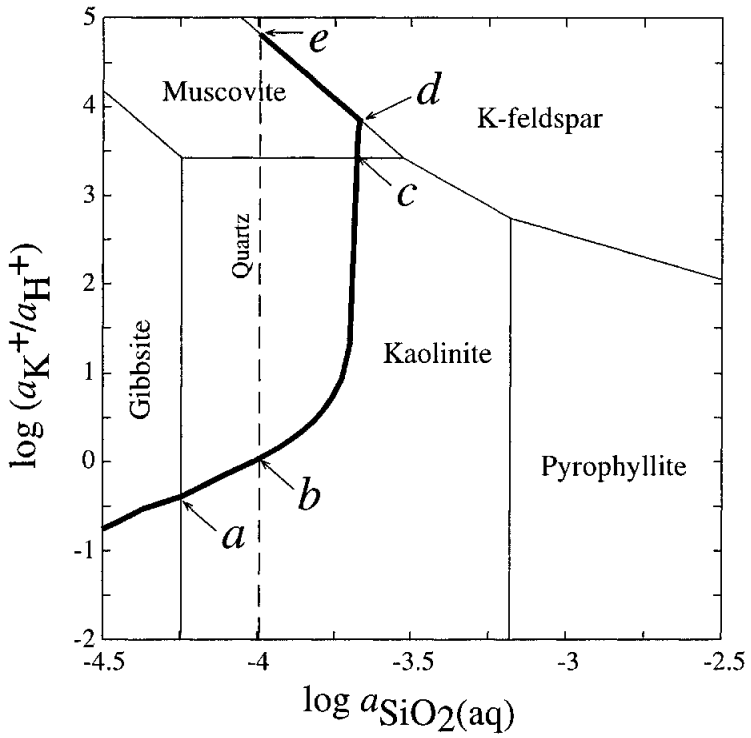

Figure 10: Reaction path (bold curve) representing interaction of a granitic rock consisting of K-feldspar and quartz with acidic groundwater at 25°C, plotted on an activity-activity diagram for the system K_2O-Al_2O_3-SiO_2-H_2O.

The time evolution of the reaction path is represented in Fig. 11 in terms of the residence time (equivalent to reaction-path time) and saturation indices for K-feldspar, quartz, gibbsite, kaolinite and muscovite. Labels *a-d* refer to the events in the reaction path discussed above (the final increment of the reaction path represented by the interval *d-e* in Fig. 10 is not shown in Fig. 11, however). Negative values of the saturation index indicate the solution is undersaturated with respect to the mineral, positive values indicate it is supersaturated, and local equilibrium is indicated when the saturation index equals 0. The point labeled *a*, for example, indicates that both gibbsite and kaolinite are equilibrated with the aqueous phase, because the saturation index for both minerals is equal to zero. With increasing time, the saturation index of gibbsite turns negative, indicating that it cannot precipitate, but the saturation index of kaolinite remains equal to zero up to about 0.085 years, at which time both muscovite and kaolinite are equilibrated with the solution. With regard to the primary minerals in granite, it can be seen that K-feldspar closely approaches equilibrium after about 0.125 years, but the solution remains supersaturated with respect to quartz at times exceeding 0.15 years.

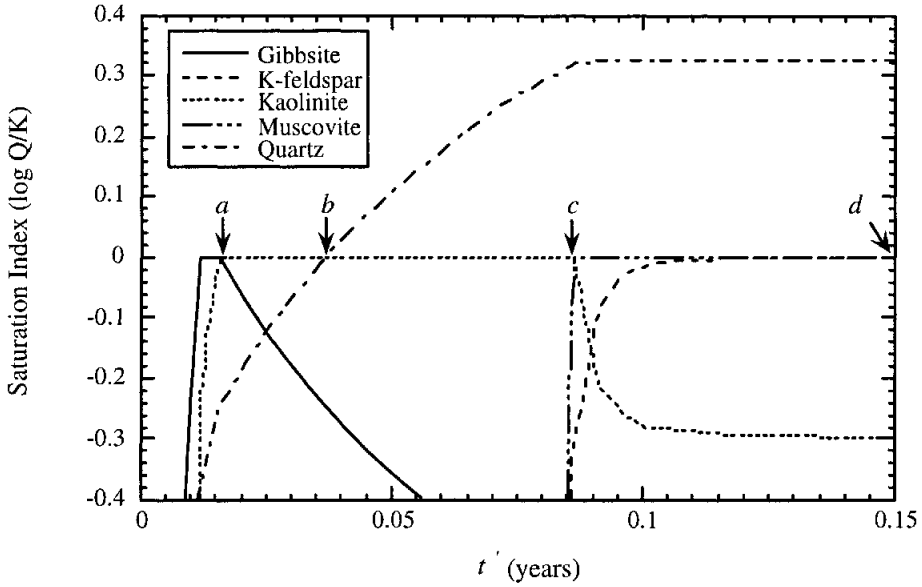

Figure 11: Variations in mineral saturation indices associated with the alteration of granite by an acidic groundwater as a function of the residence time of the groundwater in the flow path (see text).

The time evolution of the reaction path is transformed into spatial coordinates using Eqn. (25), with v/ϕ = 100 m yr^{-1}. Results are shown in Fig. 12. Associated spatial variations in solution chemistry are used in the following section to estimate attenuation parameters for the pH front.

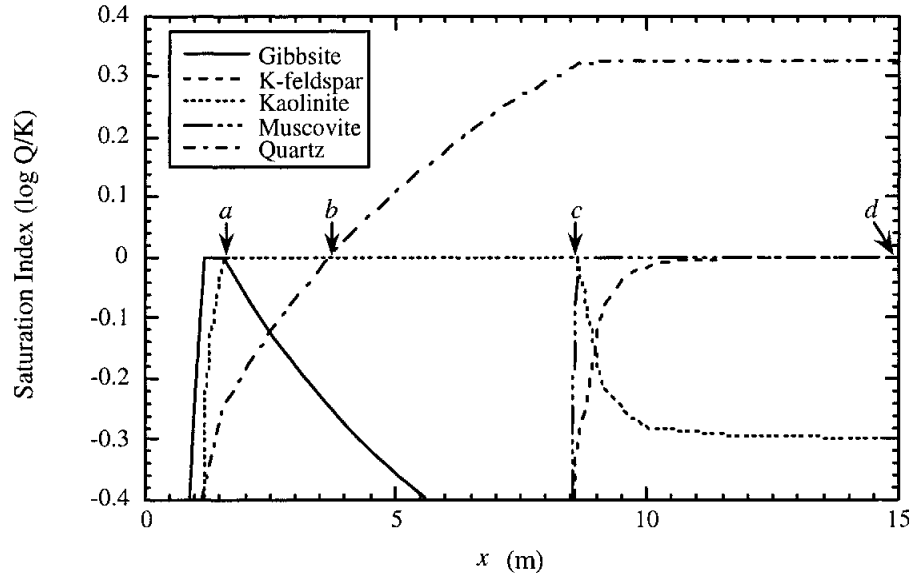

Figure 12: Variations in mineral saturation indices associated with the alteration of granite by an acidic groundwater as a function of location in the flow path (see text).

3.2.3 Analytical solution

Results of the reaction-path calculation described in Section 3.2.2 that fix the migration velocity of the corresponding pH front are shown in Fig. 13. As can be seen, pH is calculated to vary from pH 4 at the inlet (x = 0) to about pH 7.8, 9 m downstream. Also

shown in the figure are associated variations in K^+ concentrations, ranging from about 10^{-10} mol kg^{-1} at the inlet to $10^{-3.98}$ mol kg^{-1} 8.5 m downstream. The latter value corresponds to equilibration of the evolved solution composition with respect to K-feldspar. As can be seen in the figure, the location in the flowpath where this occurs is nearly coincident with the position of a sharp pH front separating a downstream region where the pH is less than 5 from an upstream region where the pH is greater than 7. The position of this front is thus approximately the same as that representing the K-feldspar dissolution-equilibration front. These two fronts will moreover remain in close proximity as long as stationary state conditions prevail, because front velocities are fixed under such conditions (Lichtner, 1988).

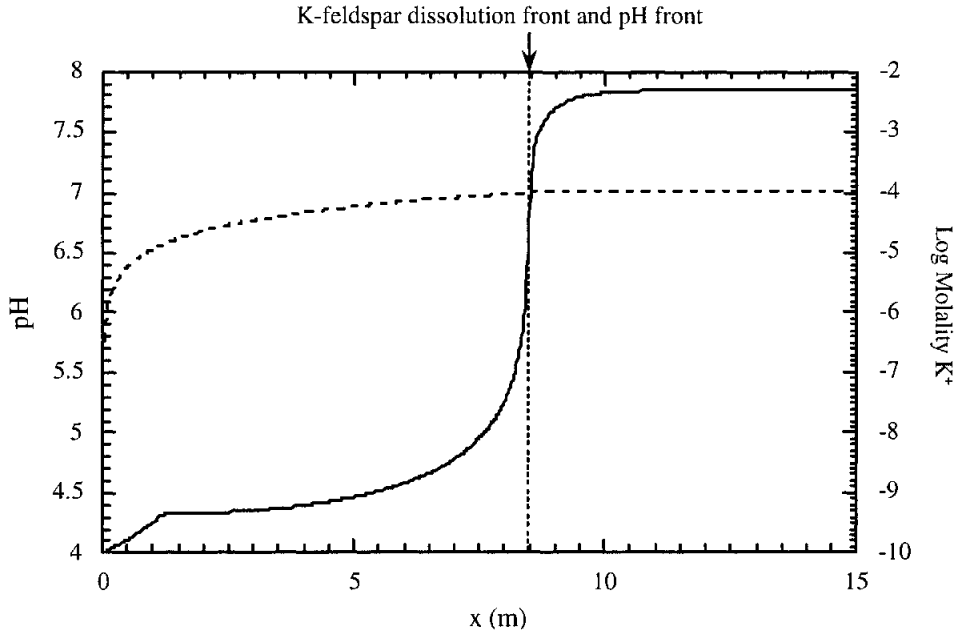

Figure 13: Calculated concentration of K^+ and pH associated with the interaction of granite with acidic groundwater as a function of location in the flow path. The location of the K-feldspar dissolution front separates regions in the flow path where K-feldspar dissolves (upstream of the front) or is equilibrated with groundwater (downstream of the front). The corresponding pH front is approximately coincident with the K-feldspar dissolution front, and migrates at the same velocity.

To estimate the migration velocity of the K-feldspar dissolution-equilibration front, and thus that of the corresponding pH front, we refer to Eqn. (53) and note that

$$\left\langle \psi_{K^+} \right\rangle = 10^{-3.98} - 10^{-10} \approx 10^{-3.98} \text{mol kg}^{-1} \approx 10^{-3.98} \text{ mol } 1000 \text{ cm}^{-3}, \text{ and}$$

$$\left\langle \phi_{K-feldspar} \right\rangle = 0.2.$$

The latter constraint in effect describes the total concentration (per unit volume of the porous medium) of K-feldspar that is available to dissolve into a packet of fluid co-located with the front. The front cannot move downstream until K-feldspar dissolves completely. The former constraint describes resultant changes in the aqueous concentration of K^+. The upper bound of this range is fixed by solubility equilibrium with respect to K-feldspar. Substituting the above values into Eqn. (53), with $V_{\text{K-feldspar}}$ = 108.87 cm^3 mol^{-1} (Robie et al., 1978), $\nu_{K+,\text{K-feldspar}} = 1$, and $\phi = 0.1$ (see Section 3.2.2),

gives the dimensionless result L_{K+} = 1.75 x 10^5. The corresponding front velocity calculated using Eqns. (52) and (51) with v = 10 m yr^{-1} is v_f = 0.57 mm yr^{-1}.

This example suggests that mineral-fluid reactions will strongly attenuate the migration of reaction fronts relative to the Darcy flow velocity. For conditions considered in this example, the velocity of the pH front is 5.7 x 10^{-5} times slower than the flow velocity. The corresponding time for the front to migrate 500 m, representing the minimum travel distance between the surface and a KBS-3 repository, is about 9 x 10^5 years. Similar results are obtained for the migration of oxidizing groundwaters in rocks containing low concentrations of ferrous minerals (Lichtner and Waber, 1992; Arthur, 1996).

3.2.4 Summary

Reaction-front velocities under stationary-state conditions will be retarded relative to the Darcy flow velocity by an amount that is inversely proportional to a "retardation factor". Such factors appear to depend on the chemical buffering properties of reactions controlling front migration, which is consistent with the suggestion by Rosing (1993) that front velocities must be inversely proportional to the buffer intensity. A geochemical modeling approach compatible with stationary-state conditions is used to estimate retardation factors controlling the migration of a pH front in a granitic host rock. Results suggest that mineral-fluid reactions will cause the front to migrate about 5 x 10^{-5} times slower than the flow velocity.

4 Summary and Conclusions

Thermodynamic and kinetic constraints on the chemical buffering properties of natural and engineered-barrier systems are derived in this report from theoretical descriptions, incorporated in the reaction-path model, of reversible and irreversible mass transfer in multicomponent, multiphase systems. The buffering properties of such systems are conditional properties because they refer to a specific aqueous species in a system that is open with respect to a specific reactant. A mathematical statement of this concept is given by Eqn. (2). A solution of this equation requires evaluation of the dependence of the activity of the buffered species on incremental changes in the overall reaction-progress variable. This dependence is represented by a truncated Taylor's series expansion [Eqn. (5)], where the values of associated derivatives are estimated using finite-difference techniques and mass-balance, charge-balance and mass-action constraints given by Eqns. (8), (12) and (17), respectively. Kinetic constraints on buffering behavior can be described if the relation between reactant flux and reaction rate is well defined. This relation is explicit for the important case of advective groundwater flow and water-rock interaction, in which case kinetic constraints on the chemical buffering properties of groundwater systems are represented by Eqn. (31).

With this theoretical background in mind, we apply the concept of chemical buffering to processes that could affect the performance of a deep geologic repository for nuclear waste. Specifically, we focus on the suggestion by Rosing (1993) that an inverse relation must exist between the buffer intensity and the migration velocity of reaction fronts in systems involving advective or diffusive mass transport. A quantitative understanding of this relation would provide the basis for evaluating the potential role of chemical buffering in achieving the isolation and retardation functions of the EBS and geosphere in a KBS-3 repository.

To evaluate this concept, we simulate the acidimetric/ alkalimetric titration of pore solutions equilibrated with water-saturated, compacted MX-80 bentonite. The inverse of derivatives of the calculated titration curve (pH versus the number of moles l^{-1} of a strong acid or strong base added to the system) provides estimates of the pH buffer intensity. Both an analytical and adaptive-grid numerical model are then used to simulate the propagation velocity of a pH front through the buffer. Two assumptions that are adopted provisionally in the models may be require additional consideration, however - 1) that the region near the pH front is a closed chemical system, and 2) that local and partial equilibrium is sustained as H^+ diffuses into this region.

A reaction-path model appropriate for advection-dominated groundwater flow in one spatial dimension is also used in this study to evaluate the inverse relation between chemical buffering due to water-rock interaction and the migration velocities of reaction fronts. The modeling approach is based on the stationary state approximation to the governing mass-transport equations controlling coupled fluid flow and water-rock interaction. A consequence of stationary-state behavior is that the migration velocity of a reaction front is fixed relative to the Darcy flow velocity. An analytical expression consistent with this behavior predicts that front velocities are attenuated relative to the flow velocity by a retardation factor, which is similar, and in some cases identical, to the buffer intensity of reactions that control the front. A key assumption in this model is that the groundwater system involves purely advective transport in a homogeneous

porous medium. This may be unrealistic in real groundwater systems, except over extremely limited scales of space and time.

Model results suggest that buffering may strongly attenuate the migration velocities of reaction fronts. For conditions considered in the bentonite model, for example, front velocities calculated using Eqn. (54) range from 6.6 x 10^{-2} to 6.6 x 10^{-5} mm yr^{-1}, corresponding to estimated values of the total buffer intensity between 1 and 1000 meq l^{-1}, respectively. Corresponding travel times for the front to migrate from the buffer-host rock interface to the buffer-canister boundary range from about 5 x 10^{3} to 5 x 10^{6} years. The lower limit of this range may correspond to weak buffering by calcite-water reactions, assuming, for example, that other mineral-fluid reactions are kinetically inhibited. The upper limit may represent strong buffering by calcite plus other reactions involving aluminosilicate phases in the buffer. Similarly, for conditions considered in the granite-weathering problem, the velocity of the pH-front is estimated to be about 5.7 x 10^{-1} mm yr^{-1}, or a factor 5.7 x 10^{-5} slower than the assumed Darcy flow velocity of 10 m yr^{-1}. The corresponding time for a pH front to migrate 500 m (*e.g.*, from the ground surface to the depth of a KBS-3 repository) is about 9 x 10^{5} years.

An important conceptual result of both the near-field and far-field models is that reaction-front velocities are inversely proportional to the buffer intensity of reactions that define the front. The effective velocity of a pH front migrating through the buffer, for example, is given by (see Section 3.1):

$$v_f = x / t_f \ , \tag{54}$$

where x stands for the thickness of the buffer, and t_f , given by Eqn. (40), or (42), represents the travel time for the front to migrate from the buffer-rock boundary to the buffer-canister boundary. Substituting Eqns. (40) or (42) into Eqn. (54) and rearranging gives the result:

$$v_f \approx \frac{x\Delta C}{5.3\beta'}, \tag{55}$$

where symbols are defined in Section 3.1. A similar equation for the case of granite interaction with an acidic groundwater is given by Eqn. (51):

$$v_f = \frac{v}{\phi R},$$

where, as noted in Section 3.2.1, the magnitude of the retardation factor, R, depends on the value of a coefficient that is equivalent, or closely similar, to the pH buffer intensity defined by the inverse of Eqn. (1). Both Eqns. (51) and (55) thus appear to confirm the suggestion by Rosing (1993) that the migration velocities of reaction fronts are inversely proportional to the buffer intensity.

The results of the present study, though preliminary, suggest that the effects of chemical buffering may play an important role in achieving the retardation and isolation functions of the EBS and geosphere in a KBS-3 repository. For example, periods of time that are significant in relation to performance-assessment time scales may be required for a pH front, and perhaps other types of fronts, to migrate from the buffer-host rock boundary

to the buffer-canister boundary (just 35 cm in width). This implies that the KBS-3 near field could in effect be decoupled from the far field, thus minimizing effects on repository performance of time-dependent variations in the geosphere. Similarly, buffering may strongly resist changes in the chemistry of the geosphere, which could be caused, for example, by future variations in climate or other natural or man-induced processes. Although the effects of such processes are difficult to accurately predict over long periods of time, they may be relatively unimportant if the effects are minimized by chemical buffering.

5 References

Anderson, G. M. and Crerar, D. A. 1993. *Thermodynamics in Geochemistry: The Equilibrium Model.* Oxford University Press, New York, New York, 588p.

Arthur, R. 1996. Estimated rates of redox-front migration in granitic rocks (SITE 94). SKI Report 96:35, Swedish Nuclear Power Inspectorate, Stockholm, Sweden.

Arthur, R. C., Savage, D., Sasamoto, H., Shibata, M. and Yui, M. 2000. Compilation of kinetic data for geochemical calculations. JNC TN8400 2000-005, Japan Nuclear Cycle Development Institute, Tokai-mura, Japan.

Balay, S., Gropp, W. D., McInnes, L. C., and Smith, B. 1997. Efficient management of parallelism in object oriented numerical software libraries. In *Modern software tools in scientific computing* (E. Arge, A. M. Bruaset and H. P. Langtangen, eds.). Birkhauser Press, 163-202.

Barnaby, R. J. and Rimstidt, J. D. 1989. Redox conditions of calcite cementation interpreted from Mn and Fe contents of authigenic calcites. *Geol. Soc. Amer. Bull.*, 101, 795-804.

Bethke, C. M. 1996. *Geochemical reaction modeling: Concepts and applications.* Oxford University Press, New York, 397p.

Bruno, J., Arcos, D. and Duro, L. 1999. Processes and features affecting the near field hydrochemistry: Groundwater-bentonite interaction. SKB TR 99-29, Swedish Nuclear Fuel and Waste Management Co., Stockholm, Sweden.

Cama, J., Ganor, J. and Lasaga, A. C. 1994. The kinetics of smectite dissolution. *Mineral. Mag.*, 58A, 140-141.

Cama, J., Ganor, J., Ayora, C. and Lasaga, A.C. 2000. Smectite dissolution kinetics at 80°C and pH 8.8. *Geochim. Cosmochim. Acta*, 64 (15), 2701-2717.

De Donder, T. 1920. *Lecons de thermodynamique et de chimie-physique.* Gauthier-Villars, Paris.

Drever, J. I. and Clow, D. W. 1994. Weathering rates in catchments. In*:* *Chemical weathering rates of silicate minerals* (A. F. White and S. L. Brantley, eds.), Rev. Mineral., 31, Min. Soc. Amer., 463 – 483.

Eckert, E.R.G., and Drake, R.M. 1972. *Analysis of Heat and Mass Transfer*, McGraw-Hill.

Eugster, H. P. 1957. Heterogeneous reactions involving oxidation and reduction at high pressures and temperatures. *Jour. Phys. Chem.*, 26, 1760-1761.

Fritz, B. and Tardy, Y. 1967a. Séquence des minéraux secondaires dans l'altération des granites et roches basiques: modéles thermodynamiques: *Bull. Soc. Geol. France*, 7, 7-12.

Fritz, B. and Tardy, Y. 1967b. Predictions of mineralogical sequences in tropical soils by a theoretical dissolution model. In: *Proceedings int. symp. on water-rock interaction* (J. Cadek and T. Paces, eds), Prague Geol. Survey, 409-416.

Furrer, G., Zysset, M. and Schindler, P. W. 1993. Weathering kinetics of montmorillonite: Investigations in batch and mixed-flow reactors. In: *Geochemistry of clay-pore fluid interactions* (D.A.C. Manning, P.T. Hughes and C. R. Hughes, eds.), Chapman & Hall, London, 243-262.

Glynn, P. and Voss, C. 1999. Geochemical characterization of Simpevarp ground waters near the Äspö Hard Rock Laboratory. SKI Report 96:29, Swedish Nuclear Power Inspectorate, Stockholm, Sweden.

Greenwood, H. J. 1975. Buffering of pore fluids by metamorphic reactions. *Am. J. Sci.*, 275, 573-593.

Guimerà, J., Duro, L., Jordana, S. and Bruno, J. 1999. Effects of ice melting and redox front migration in fractured rocks of low permeability. SKB TR 99-19, Swedish Nuclear Fuel and Waste Management Co., Stockholm, Sweden.

Helgeson, H. C. 1968. Evaluation of irreversible reactions in geochemical processes involving minerals and aqueous solutions. I: thermodynamic relations. *Geochim. Cosmochim. Acta*, 32, 853-877.

Helgeson, H. C. 1970. A chemical and thermodynamic model of ore deposition in hydrothermal systems: In *Fiftieth Anniversary Symposia* (B.A. Morgan, ed.), *Min. Soc. Am. Spec. Paper* 3, 155-186.

Helgeson, H. C. 1972. Kinetics of mass transfer among silicates and aqueous solutions: Correction and clarification *Geochim. Cosmochim. Acta*, 36, 1067-1070.

Helgeson, H. C. 1979. Mass transfer among minerals and hydrothermal solutions: In *geochemistry of hydrothermal ore deposits, 2nd ed.* (H. L. Barnes, ed.). Wiley Interscience, New York, 568-610.

Helgeson, H. C., Garrels, R. M. and MacKenzie, F. T. 1969. Evaluation of irreversible reactions in geochemical processes involving minerals and aqueous solutions – II. Applications. *Geochim. Cosmochim. Acta*, 33, 455-481.

Helgeson, H. C., Brown, T. H., Nigrini, A. and Jones, T.A. 1970. Calculation of mass transfer in geochemical processes involving aqueous solutions *Geochim. Cosmochim. Acta*, 34, 569-592.

Heydemann, A. 1966. Über die chemische verwitterung von tonmineralen (experimentelle untersuchungen). *Geochim. Cosmochim. Acta*, 30, 995-1035.

Hutcheon, I. Shevalier, M. and Abercrombie, H. J. 1993. pH buffering by metastable mineral-fluid equilibria and evolution of carbon dioxide fugacity during burial diagenesis. *Geochim. Cosmochim. Acta*, 57, 1017-1027.

Jørgensen, H. 1955. Om definitionen af begrebet "Puffer" (Stodpude). *Kemisk månedsblad*, 36, 45-52.

Kittrick, J. A. 1979. Ion exchange and mineral stability: Are the reactions linked or separate? in *Chemical modeling in aqueous systems* (E. A. Jenne, ed.), *Am. Chem. Soc. Symp. Series*, Washington, D. C., 401-412.

Lichtner, P. C. 1985. Continuum model for simultaneous chemical reactions and mass transport in hydrothermal systems. *Geochim. Cosmochim. Acta*, 49, 779-800.

Lichtner, P. C. 1988. The quasi-stationary state approximation to coupled mass transport and fluid-rock interaction in a porous medium. *Geochim. Cosmochim. Acta*, 52, 143-165.

Lichtner, P. C. and Waber, N. 1992. Redox front geochemistry and weathering: Theory and application to the Osamu Utsumi uranium mine, Poços de Caldas, Brazil. *Jour. Geochem. Explor.*, 45, (1/3), 521-564.

May, H. M., Kinniburgh, D. G., Helmke, P. A. and Jackson, M. L. 1986. Aqueous dissolution, solubilities and thermodynamic stabilities of common aluminosilicate clay minerals: Kaolinite and smectites. *Geochim. Cosmochim. Acta*, 50, 1667-1677.

McKinley, I. and Savage, D. 1994. Comparison of solubility databases used for HLW performance assessment. *Radiochim. Acta*, Fourth International Conference on the Chemistry and Migration Behavior of Actinides and Fission Products in the Geosphere, Charleston, SC USA, Dec. 12-17, 1993, 657-665.

Murphy, W. M. and Helgeson, H. C. 1989. Thermodynamic and kinetic constraints on reaction rates among minerals and aqueous solutions. IV. Retrieval of rate constants and activation parameters for the hydrolysis of pyroxene, wollastonite, olivine, andalusite, quartz, and nepheline. *Am J. Sci.*, 289, 17-101.

Nagy, K. L. 1994. Dissolution and precipitation kinetics of sheet silicates. In: *Chemical weathering rates of silicate minerals* (A. F. White and S. L. Brantley, eds.), Rev. Mineral., 31, Min. Soc. Amer., 173-233.

Neretnieks, I. 1985. Some aspects of the use of iron canisters in deep lying repositories for nuclear waste. Nagra TR 85-35, Baden, Switzerland.

Ortoleva, P., Auchmuty, G., Chadam, J., Hettmer, J., Merino, E., Moore, C. H. and Ripley, E. 1986. Redox front propagation and banding modalities. *Physica*, 19D, 334-354.

Prigogine, I. 1955. *Introduction to thermodynamics of irreversible processes*. Wiley, New York.

Roaldset, E. G., Sällfors, G. and Arthur, R. 1996. Förstudie beträfande bentonitens roll i ett slutförvar för radioaktivt avfall (feasibility study of the role of bentonite in a

radioactive waste repository). SKI Report 96:44, Swedish Nuclear Power Inspectorate, Stockholm, Sweden (in Swedish).

Robie, R. A., Hemingway, B. S. and Fisher, J. R. 1978. Thermodynamic properties of minerals and related substances at 298.15 °K and 1 bar (10^5 pascals) pressure and at higher temperatures. *U.S. Geol. Surv. Bull.*, 1452, 456p.

Robinson, P. 1998. personal communication.

Rosing, M. 1993. The buffering capacity of open heterogeneous systems. *Geochim. Cosmochim. Acta*, 57, 2223-2226.

Savage, D., Arthur, R. C. and Saito, S. 1999. Geochemical factors in the selection and assessment of sites for the deep disposal of radioactive wastes. In: *Chemical containment of waste in the geosphere* (R. Metcalfe and C. A. Rochelle, eds.), Geological Society, London, Spec. Pubs. 157, 27-45.

Sørensen, S. P. L. 1909. Enzymstudier II. *Medd. Carlsberg Laboratoriet*, 8, 1 – 168.

SKB 1992. SKB 91: Final disposal of spent nuclear fuel. Importance of the bedrock for safety. SKB TR 92-20, Swedish Nuclear Fuel and Waste Management Co., Stockholm, Sweden.

SKB 1995. Treatment and final disposal of nuclear waste: Programme for encapsulation, deep geologic disposal, and research, development and demonstration. SKB RD&D-Programme 95, Swedish Nuclear Fuel and Waste Management Co., Stockholm, Sweden.

SKB 1999. SR-97 – Post-closure safety: Deep repository for spent nuclear fuel. SKB TR 99-06, Swedish Nuclear Fuel and Waste Management Co., Stockholm, Sweden.

SKI 1996. SKI Site – 94: Deep repository performance assessment project. SKI Report 96:36, Swedish Nuclear Power Inspectorate, Stockholm, Sweden.

Stumm, W. and Morgan, J. J. 1996. *Aquatic Chemistry, 3rd ed.* Wiley Interscience, New York.

Van Slyke, D. D. 1922. On the measurement of buffer values and on the relationship of buffer values to the dissociation constant of the buffer and the concentration and reaction of the buffer solution. *J. Biol. Chem.*, 52, 525-570.

Wanner, H., Wersin, P. and Sierro, N. 1992. Thermodynamic modeling of bentonite-groundwater interaction and implications for near field chemistry in a repository for spent fuel. SKB TR 92-37, Swedish Nuclear Fuel and Waste Management Co., Stockholm, Sweden.

Wieland, E., Wanner, H., Albinsson, Y., Wersin, P. and Karnland, O. 1994. A surface chemical model of the bentonite-water interface and its implications for modelling the near field chemistry in a repository for spent fuel. SKB TR 94-36, Swedish Nuclear Fuel and Waste Management Co., Stockholm, Sweden.

Wolery, T. J. 1978. Some chemical aspects of hydrothermal processes at mid-ocean ridges – a theoretical study: I Basalt-sea water reaction and chemical cycling between the oceanic crust and the oceans. II. Calculation of chemical equilibrium between aqueous solutions and minerals. Ph.D. thesis, Northwestern University, Evanston, Ill.

Wolery, T. J. 1992. EQ3/6, a software package for geochemical modeling of aqueous systems: Package overview and installation guide. UCRL-MA-110662 PT I, Lawrence Livermore National Laboratory, Livermore, CA.